# Rock magnetism of remagnetized carbonate rocks: another look

MIKE JACKSON* & NICHOLAS L. SWANSON-HYSELL

*Institute for Rock Magnetism, Winchell School of Earth Sciences, University of Minnesota, Minnesota, US*

**Corresponding author (e-mail: jacks057@umn.edu)*

**Abstract:** Authigenic formation of fine-grained magnetite is responsible for widespread chemical remagnetization of many carbonate rocks. Authigenic magnetite grains, dominantly in the superparamagnetic and stable single-domain size range, also give rise to distinctive rock-magnetic properties, now commonly used as a 'fingerprint' of remagnetization. We re-examine the basis of this association in terms of magnetic mineralogy and particle-size distribution in remagnetized carbonates having these characteristic rock-magnetic properties, including 'wasp-waisted' hysteresis loops, high ratios of anhysteretic remanence to saturation remanence and frequency-dependent susceptibility. New measurements on samples from the Helderberg Group allow us to quantify the proportions of superparamagnetic, stable single-domain and larger grains, and to evaluate the mineralogical composition of the remanence carriers. The dominant magnetic phase is magnetite-like, with sufficient impurity to completely suppress the Verwey transition. Particle sizes are extremely fine: approximately 75% of the total magnetite content is superparamagnetic at room temperature and almost all of the rest is stable single-domain. Although it has been proposed that the single-domain magnetite in these remagnetized carbonates lacks shape anisotropy (and is therefore controlled by cubic magnetocrystalline anisotropy), we have found strong experimental evidence that cubic anisotropy is not an important underlying factor in the rock-magnetic signature of chemical remagnetization.

The usefulness of a palaeomagnetic remanence is directly related to the accuracy with which its age is known (e.g. Van der Voo 1990). Primary remanence, acquired during or very soon after rock formation, provides direct information on palaeofield orientation and strength at that time. The possibility of partial or complete remagnetization at a later time complicates palaeomagnetic interpretation, as has long been recognized (e.g. Graham 1949). Every robust palaeomagnetic study must therefore include some effort to constrain the ages of identified components of the natural remanent magnetization (NRM). Relative dating with respect to sedimentary processes, structural tilting or cross-cutting relationships is the basis of the classical geometric palaeomagnetic tests (fold test and conglomerate test, Graham 1949; baked contact test, Everitt & Clegg 1962; unconformity test, Kirschvink 1978). The special circumstances required for application of these tests are often not available however, or positive test results may provide relatively loose constraints allowing magnetization ages that significantly post-date the age of the rock formation. As a result, other evidence (although generally more indirect) becomes essential in evaluating the age, origin and significance of NRM components. Such evidence commonly includes petrographic observations, isotopic and geochemical data and rock magnetic characterization.

By their very existence, magnetic overprints provide evidence of some process or event of potential geological significance (e.g. McCabe & Elmore 1989; Elmore & McCabe 1991). The 'usual suspects' in remagnetization are a set of mechanisms involving elevated temperature, stress and chemical activity, acting alone or in concert, and producing changes in the magnetic minerals themselves and/or in the remanence that they carry. When the NRM and the population of magnetic carriers are both modified by some process or event, careful rock magnetic analysis may shed light on the culprit.

Our focus here is chemically remagnetized carbonate rocks where any primary remanence is completely obscured by ancient yet secondary magnetizations. Many such units have been documented in recent decades (e.g. McCabe & Elmore 1989). With the advent of superconducting magnetometers in the 1970s and 1980s (Goree & Fuller 1976), carbonate rocks represented a new frontier for palaeomagnetic research. These and other weakly magnetic sedimentary rock strata had been unmeasurable during progressive demagnetization with the limited-sensitivity spinner magnetometers then available. Superconducting magnetometers enabled a rapid expansion into these untapped palaeomagnetic archives, but by the mid 1980s it was already evident that many Palaeozoic carbonate rocks had been completely remagnetized in late Palaeozoic time and it became important to understand the processes responsible (e.g. McCabe & Elmore 1989).

*From*: Elmore, R. D., Muxworthy, A. R., Aldana, M. M. & Mena, M. (eds) 2012. *Remagnetization and Chemical Alteration of Sedimentary Rocks*. Geological Society, London, Special Publications, **371**, http://dx.doi.org/10.1144/SP371.3 

## Review of previous work

### *Origins of the secondary remanence and its carriers*

Widespread remagnetization of Palaeozoic carbonate strata in the Appalachian Basin was initially recognized and documented through combined palaeomagnetic, structural and petrographic observations. These observations included the recognition that the characteristic remanent magnetization (ChRM) directions sometimes clustered significantly more tightly prior to correction for structural tilting, and sometimes clustered most tightly at intermediate unfolding. This led to interpretations that the magnetizations were acquired after and/or during folding (McCabe & Elmore 1989). Petrographic work led to the observation of spheroidal, botryoidal and framboidal magnetite grains of pure end-member $Fe_3O_4$ composition that were interpreted to be of low-temperature diagenetic origin (McCabe *et al.* 1983). Early rock-magnetic characterization focused on acquisition and demagnetization of isothermal remanent magnetization (IRM) and anhysteretic remanent magnetization (ARM), leading in many cases to the conclusion that the remanence carriers were dominantly pseudo-single-domain (PSD) or multi-domain (MD) magnetite (e.g. McElhinny & Opdyke 1973; Kent 1979). Hysteresis measurements eventually led to the recognition that the dominant magnetic carriers in many remagnetized carbonates are in fact very fine grained, mainly in the superparamagnetic (SP) and stable single-domain (SSD) size range (Jackson 1990; McCabe & Channell 1994; Suk & Halgedahl 1996; Dunlop 2002*b*). Moreover, the high proportions of SP and SSD particles in the ferrimagnetic inventory of these rocks result in unusual combinations of the summary parameters conventionally used to represent hysteresis behaviour, namely coercivity $B_c$, remanent coercivity $B_{cr}$, saturation magnetization $M_s$, saturation remanence $M_{rs}$ and the ratios $B_{cr}/B_c$ and $M_{rs}/M_s$. On the 'Day plot' ($M_{rs}/M_s$ v. $B_{cr}/B_c$; Day *et al.* 1977; Dunlop 2002*a*, *b*), remagnetized carbonates are largely isolated in a region that is distinct from the regions occupied by most other rocks, sediments and synthetic materials (Fig. 1), leading to the suggestion that hysteresis properties could be used as a fingerprint for recognition of remagnetized strata (Jackson 1990; Channell & McCabe 1994; McCabe & Channell 1994). We will explore the basis and the limitations of this idea in some depth in the present paper.

The origin of the ancient yet secondary characteristic remanence was attributed by McCabe *et al.* (1983) to chemical processes (growth of new minerals and/or replacement of pre-existing minerals). The spatial/temporal association of widespread remagnetization with Appalachian–Alleghenian–Variscan–Hercynian orogenesis (for summaries see e.g. Weil & Van der Voo 2002; Tohver *et al.* 2008) soon led to various hypotheses involving continental-scale flow of orogenic fluids (Oliver 1986; Bethke & Marshak 1990; Garven 1995) to account for not only remagnetization, but also ore mineralization and hydrocarbon distribution in a number of different basins. Isotopic and geochemical evidence in some cases ruled out a significant role for exotic brines (e.g. Elmore *et al.* 1993; Ripperdan *et al.* 1998), and pointed instead to more closed-system mechanisms including clay diagenesis (Katz *et al.* 2000; Woods *et al.* 2002), organic maturation (Blumstein *et al.* 2004) and pressure solution (Zegers *et al.* 2003; Elmore *et al.* 2006; Oliva-Urcia *et al.* 2008). Kent (1985) questioned whether the remagnetization necessarily involved chemical mechanisms at all, suggesting that viscous acquisition during the Kiaman superchron was a viable alternative. Noting that the range of observed unblocking temperatures could be accounted for by the Viscous Remanent Magnetization (VRM) model of Walton (1980), Kent (1985) demonstrated moreover that the Brunhes-aged viscous overprint in these rocks had unblocking temperatures similar to those predicted by the same model. However, this model was later shown to be inappropriate for predicting unblocking temperatures (Dunlop *et al.* 1997*a*, *b*), undermining the theoretical basis for a viscous origin but not the empirical observations. Similarly, Kligfield & Channell (1981) invoked thermoviscous mechanisms to explain widespread Brunhes-age remagnetization of limestones from the Swiss Alps, in which the ChRM was carried chiefly by pyrrhotite with fine grain sizes spanning the SP–SSD range. They noted that the pyrrhotite may have formed by alteration of early-diagenetic pyrite, but did not address the possibility of a chemical origin for the remanence.

Subsequent work on the remagnetized Appalachian Basin carbonates and remagnetized carbonates in other basins has largely supported the idea that the remanence carriers are predominantly of late diagenetic origin, and that one or more chemical mechanisms were involved in producing the secondary characteristic components of natural remanence (Reynolds 1990; Suk *et al.* 1990*a*, *b*, 1991, 1993; Weil & Van der Voo 2002; Zwing *et al.* 2005). Our focus here is on the important role that rock magnetic studies have played in the understanding of carbonate remagnetization, but of course we recognize that a complete picture also includes careful petrographic, geochemical, isotopic, microstructural and analytical microscopic work (Elmore & McCabe 1991; Elmore 2001).

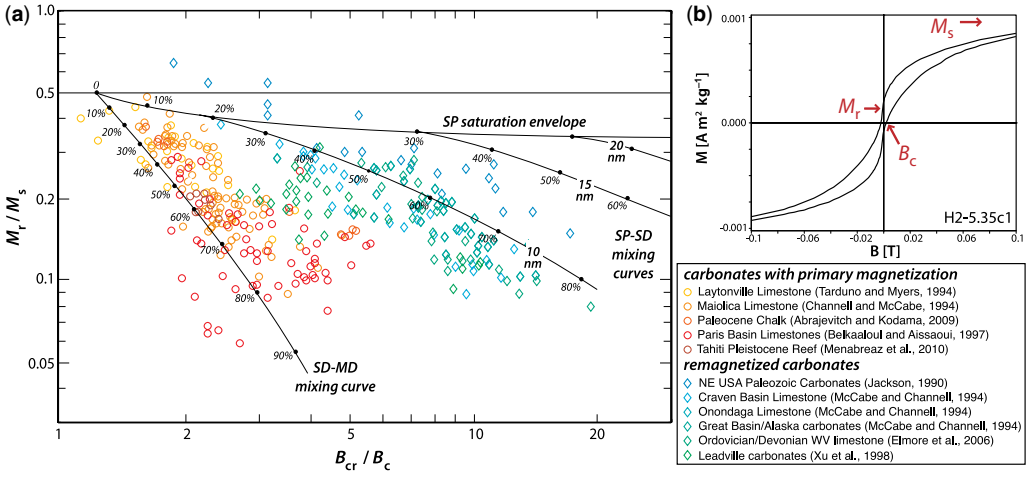


**Fig. 1.** (**a**) Summary Day plot of published hysteresis parameters for carbonate rocks, in which the ratio of remanent coercivity ($B_{cr}$) to coercivity ($B_c$) is plotted against the ratio of saturation remanence ($M_r$) to saturation magnetization ($M_s$). Data from carbonates interpreted to carry primary remanence are marked with circles, and data from carbonates interpreted to be remagnetized are marked with diamonds. (**b**) An example hysteresis loop from sample H2-5.35 of the Manlius Formation of the Helderberg Group is shown with $B_c$, $M_r$ and $M_s$ marked. Note that the loop had not reached saturation by 100 mT (the maximum of the *x*-axis), such that $M_s$ is not reached until higher applied fields (off the plot).

In the interest of clarity, we will take a specific and limited set of previously studied remagnetized carbonate units from the Appalachian Basin as prototypes of the distinctive set of rock-magnetic properties and NRM characteristics that we wish to understand. These include the Devonian Onondaga Limestone (Kent 1979; Jackson *et al.* 1988; Suk *et al.* 1990*a*; Lu *et al.* 1991) and Helderberg Group (Scotese *et al.* 1982) and the Ordovician Trenton Limestone (McElhinny & Opdyke 1973; McCabe *et al.* 1984) and Knox Dolomite (Bachtadse *et al.* 1987; Suk *et al.* 1990*b*). All of these carry a two-component NRM with a well-documented reverse-polarity Permian-aged ChRM and a normal-polarity recent viscous overprint, and all exhibit rock-magnetic properties dominated by SP and SSD ferrimagnets (Jackson 1990; Jackson *et al.* 1993; Jackson & Worm 2001; Dunlop 2002*b*). By understanding as well as possible the relationship between the ChRM and the magnetic phases and their origins in these prototypical units, our goal is to improve our ability to interpret similarities and differences in properties observed in other carbonate strata for which the magnetization history is less well known.

## *Unresolved questions*

*Nature of grain-scale anisotropy.* The hysteresis ratios of several of the remagnetized Palaeozoic carbonate units from the Appalachian Basin follow a power-law trend, visible as a linear array of points on a bilogarithmic Day plot as in Figure 1. This trend is best explained as resulting from a mixture of SP and SSD ferrimagnets (Dunlop 2002*a*, *b*). Further, it has been suggested (Jackson 1990) that the SSD fraction (at least) in remagnetized Appalachian carbonates has properties dominated by cubic magnetocrystalline (multiaxial) anisotropy rather than by shape anisotropy. In a population of randomly oriented single-domain ferrimagnetic particles dominated by uniaxial shape anisotropy, the ratio $M_r/M_s$ should approach 0.5 as the coercivitiy ratio approaches 1 (Stoner & Wohlfarth 1948). In contrast, the $M_r/M_s$ intercept for the remagnetized Appalachian carbonates is *c.* 0.89, as expected for randomly oriented single-domain (SD) grains with cubic anisotropy (Wohlfarth & Tonge 1957). It should be noted that the error bars on this intercept value are relatively large, and moreover that linear extrapolation is probably not valid (Dunlop 2002*a*, *b*). Nevertheless, the suggestion of dominantly cubic anisotropy is interesting and has important implications. Populations of ferrimagnetic grains that are dominated by multiaxial anisotropy are unusual in nature, because even a slight elongation (e.g. length to width ratio of *c.* 1.1 and greater) is sufficient to make magnetostatic (shape) anisotropy the dominant factor controlling the hysteresis and remanence behaviour of magnetite or maghemite. The strong implication of a nearly complete lack of particle elongation is that the remanence-carrying

particles have authigenic/diagenetic morphologies similar to those observed for the much larger particles retrieved by magnetic extraction of insoluble residues (e.g. McCabe *et al.* 1983) and that the unobserved, much finer, SSD particles originated in the same way.

On the basis of hysteresis parameters, a similar argument for multiaxial anisotropy was later made by Gee & Kent (1995) for mid-ocean-ridge basalts (MORB), whose remanence resides chiefly in titanomagnetites of composition $Fe_{3-x}Ti_xO_4$ with $x$ *c.* 0.6 (TM60). This argument has been criticized by Fabian (2006) on two grounds. First, theoretical considerations, combined with known intrinsic material properties, suggest that cubic magnetocrystalline (multiaxial) anisotropy should almost always be less important than magnetostrictive and shape (uniaxial) anisotropies for titanomagnetites. Second, careful measurements showed that magnetization of MORB samples is often not fully saturated in the field range used for hysteresis loop measurements (typically not exceeding 1 Tesla (T), and incomplete saturation in combination with conventional linear high-field slope calculations yield erroneously low values for $M_s$ (and thus erroneously high $M_r/M_s$ ratios). Fabian (2006) showed for several MORB samples that even although loops measured on a vibrating-sample magnetometer (with peak fields of 1 T) yielded apparent $M_r/M_s$ ratios well above 0.5, measurement of the same samples in fields up to 7 T in a superconducting magnet resulted in significantly higher $M_s$ estimates and $M_r/M_s$ ratios below the uniaxial limit. Fabian (2006) concluded that uniaxial stress anisotropy exerts the dominant control on the hysteresis behaviour of MORBs. Although he did not discuss remagnetized carbonates, his findings raised questions about the identification of multiaxial anisotropy in any material through standard hysteresis experimental protocols.

Fabian's (2006) arguments and experimental results appeared conclusive, but the potential importance of magnetocrystalline anisotropy in MORBs has not been put to rest. A strong counterargument in favour of such multiaxial anisotropy in MORB titanomagnetites was recently made by Lanci (2010), by means of a clever technique based on measurements of field-impressed anisotropy of susceptibility (illustrated in Fig. 2a). The essence of Lanci's approach involves the 'inverse' anisotropy of magnetic susceptibility (AMS) of SD particles: an individual SD grain has minimum (essentially zero) susceptibility parallel to its remanent moment (because it is already magnetized to saturation in that direction) and maximum susceptibility perpendicular to that easy axis. For a population of uniaxial SD grains this results in the well-known 'inverse-fabric' effect (Potter & Stephenson 1988); a preferential alignment of long axes gives minimum susceptibility parallel to lineation. When uniaxial particles are randomly oriented, the acquisition of a strong-field remanence has only very weak effects on AMS, because particle moments are spread out all over the directional hemisphere around the net remanence (i.e. around the applied field orientation). Lanci's (2010) idea is that multiaxial particle anisotropy makes remanence effects much more extreme: even if easy axes are randomly oriented, acquisition of a strong-field remanence causes the particle moments to be confined to a much smaller range of orientations close to the applied field direction because there are more easy axes per particle. This therefore becomes the minimum susceptibility direction (Fig. 2a). Very large anisotropies of 200–300% can be produced by acquisition of a saturation isothermal remanent magnetization (SIRM) in populations of randomly oriented SD grains with multiaxial anisotropy. Lanci's experimental results showed that imprinting a 1 T IRM on several MORB samples with very weak initial AMS resulted in a strong anisotropy of susceptibility (10–25%) with $k_{min}$ parallel to the IRM, and showed that the effect could be erased by tumbling alternating-field (AF) demagnetization. He calculated that 20–30% of the susceptibility in those MORB samples can be attributed to titanomagnetite particles with multiaxial anisotropy.

Further evidence for multiaxial anisotropy in MORB samples has been presented by Mitra *et al.* (2011) using another novel experimental approach, involving asymmetry of forward and reverse IRM acquisition (illustrated in Fig. 2b). An individual uniaxial SD grain has the same switching threshold in fields of either polarity. A population of uniaxial SD grains, initially in a weakly magnetized state (e.g. NRM state, or after tumbling AF), will acquire an IRM of intensity $M_r^+$ in a non-saturating applied field $B_{app}$. Application of an equal-strength field in the opposite direction will produce an IRM of equal intensity ($M_r^- = M_r^+$) antiparallel to the positive-field IRM, as each uniaxial particle that reversed its moment into alignment with the positive field reverses again into alignment with the negative field. This equivalence between the $M_r^-$ and $M_r^+$ does not hold for multiaxial SD grains (Fig. 2b). In contrast to uniaxial grains where the moment is confined to the long axis of the grain and only two possible remanent orientations exist, multiaxial grain moments have a number of possible remanent orientations only one of which is antiparallel to the original moment orientation. Application of a non-saturating field may cause the moment of a particular grain to jump from one easy axis to another, closer to the applied field direction and thus contributing to $M_r^+$. Subsequent application of a reverse

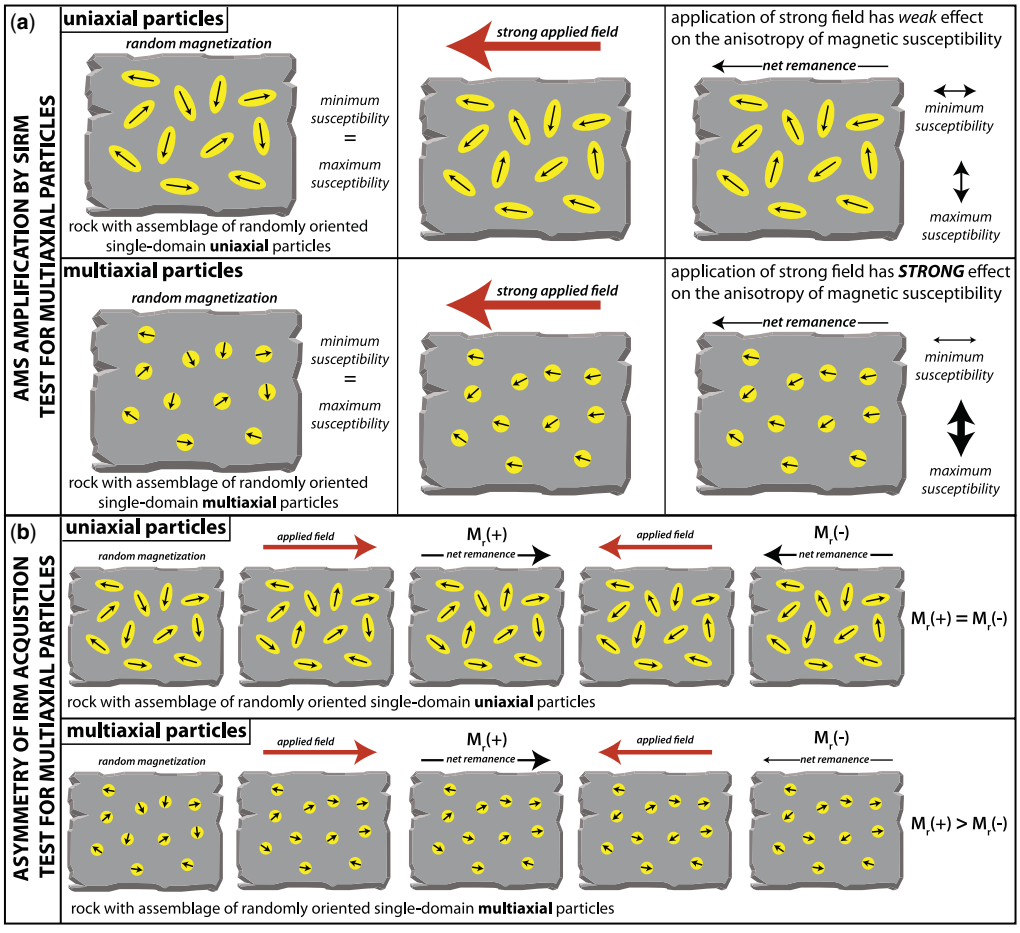


**Fig. 2.** Schematic illustration of tests for multiaxial particle anisotropy in single-domain populations. The test depicted in (**a**) involves the effects of strong-field remanence acquisition on anisotropy of low-field susceptibility (Lanci 2010); with multiaxial particle anisotropy, a strong alignment of particle moments results in a strong anisotropy of magnetic susceptibility (AMS). The test depicted in (**b**) involves asymmetric stepwise acquisition of isothermal remanent magnetization (IRM) in positive and negative fields of equal strength (Mitra *et al.* 2011). See text for detailed explanation of both tests.

field of equal strength to the population of multiaxial grains will not necessarily cause the moment of the same grain to reorient, because the angle between the moment and the field is now more acute than it was in the initial state. $M_r^-$ is consequently of lower intensity than $M_r^+$ for equal and opposite applied non-saturating fields (Fig. 2b). Mitra *et al.* (2011) demonstrated such positive/negative asymmetry in IRM acquisition experiments for MORB samples and for hematite samples (with multiaxial basal-plane grain-scale anisotropy) with intensity differences reaching 100% for intermediate applied fields, decreasing to zero for saturating fields. Similar measurements on other control samples showed essentially identical forward and reverse IRM acquisition, as expected for samples with uniaxial remanence carriers.

Although these arguments over multiaxial anisotropy have focused almost entirely on MORB samples, the same questions apply to remagnetized carbonates. Suk & Halgedahl (1996) pointed out that observed coercivities of remagnetized Applachian Basin carbonates were two to three times higher than can be theoretically produced by magnetocrystalline anisotropy in magnetite, but they suggested that a mixture of uniaxial and multiaxial particles could account for all observed properties. Evidence for multiaxial grain-scale anisotropy comes almost entirely from the intercept value of the trend line on the bilogarithmic Day plot; few

individual loops have yielded remanence ratios above 0.5 and, for those, non-saturation may be a problem. Moreover, no independent evidence for multiaxial anisotropy has been found for carbonate rocks. One goal of the present study is to apply the new techniques of Lanci (2010) and Mitra *et al.* (2011) to some of the well-studied Palaeozoic carbonates of the Appalachian Basin, to test the hypothesis that multiaxial anisotropy is a characteristic feature of their magnetic mineralogy.

*Mineral mixtures and the importance of pyrrhotite.* Wasp-waisted hysteresis loops and Day plot trends similar to those of the remagnetized carbonates in Figure 1 require the presence of two or more distinct coercivity fractions, which may correspond to either different remanence-carrying minerals with strongly contrasting coercivities (Jackson *et al.* 1990; Muttoni 1995; Roberts *et al.* 1995) or different size fractions of a single mineral (especially if one is superparamagnetic; Tauxe *et al.* 1996; Dunlop 2002*a*, *b*; Lanci & Kent 2003). These two scenarios have different implications for the origins of the carriers and, correspondingly, of the natural remanence. A single process or remagnetization event could account for the co-occurrence of SP and SSD magnetites in chemically overprinted rocks, with a unimodal size distribution of monogenetic carriers naturally producing the strong coercivity contrast (Lanci & Kent 2003). Polymineralic carrier populations imply a more complicated history where either a primary phase was preserved with a secondary authigenic phase, or where there are multiple preserved generations of secondary authigenic phases.

The magnetic mineralogy of many previously studied remagnetized carbonates is thought to comprise primarily magnetite, largely on the basis of unblocking temperatures, but remains incompletely known. In some cases pyrrhotite (Xu *et al.* 1998; Zegers *et al.* 2003) or hematite (see list in McCabe & Elmore 1989) have been documented as overprint carriers. Multiple studies have argued for the preservation of primary magnetite remanence in carbonates that have a secondary remanence held by pyrrhotite (Muttoni & Kent 1994; Symons *et al.* 2010). Strong-field thermomagnetic data are generally rare, due to the difficulty of obtaining measurable signals from small quantities of this weakly magnetic material. While a thermomagnetic curve on a sample chip of the Manlius Formation of the Helderberg Group revealed a smooth reversible curve with a Curie temperature at *c.* 565 °C (Scotese *et al.* 1982), this result has not been confirmed for other remagnetized carbonates or for other Helderberg Group samples. Laboratory heating also typically results in some degree of alteration of the magnetic mineralogy, especially for pyrrhotite and other sulphides, adding uncertainty to the interpretation. More readily measurable unblocking temperature spectra of NRM and of artificial remanences have generally shown low-to-moderate thermal stability, with typical median demagnetization temperatures (i.e. temperatures required to erase half the initial remanence) of 200–300 °C and maximum unblocking temperatures *c.* 450–500 °C (e.g. Jackson *et al.* 1993; Zegers *et al.* 2003; Elmore *et al.* 2006). These data allow multiple possibilities, including (but not requiring) significant contributions from pyrrhotite or detrital titanomagnetites as well as fine-grained pure magnetite (with $T_{ub} < T_c$) and/or magnetite with dominantly magnetocrystalline anisotropy.

Low-temperature remanence measurements (Jackson *et al.* 1993) on samples of the Devonian Onondaga Limestone and Ordovician Trenton Limeston of New York and of the Ordovician Knox Dolomite have shown a general absence of clear transitions, but subtle indications have been found in some samples of the magnetite Verwey transition ($T_v$ *c.* 120 K) (Verwey & Haayman 1941; Walz 2002) and/or of the pyrrhotite Besnus transition ($T_{Bs}$ *c.* 32 K) (Besnus 1966; Dekkers *et al.* 1989; Rochette *et al.* 1990). As has long been known (Verwey & Haayman 1941; Özdemir *et al.* 1993; Walz 2002; Özdemir & Dunlop 2010), the Verwey transition is very sensitive to deviations from perfect stoichiometry. Small degrees of cation substitution or moderate cation deficiency (due to low-temperature oxidation) depress the transition temperature and diminish the changes in measurable physical properties, and the transition is entirely suppressed by just a few percent content of substituted metal cations or vacancies due to high-temperature oxidation (Verwey & Haayman 1941). Low-temperature oxidation produces a maghemite shell on a stoichiometric magnetite core, and some expression of the Verwey transition persists to high overall degrees of oxidation (Özdemir & Dunlop 2010). The variables controlling the Besnus transition are much less well known, and even its fundamental mechanism remained unclear until quite recently (Wolfers *et al.* 2011). Nevertheless, there is a clear grain-size dependence of the magnetic behaviour across the transition. The drop in magnetization (or susceptibility) on cooling through $T_{Bs}$ increases strongly with increasing particle size, and the fractional recovery of remanence on rewarming through the transition is greater for the finer sizes (Dekkers *et al.* 1989). The smallest fraction studied by Dekkers *et al.* (1989) was 0–5 μm and for this fraction the drop in remanence on cooling across $T_{Bs}$ was about 15% of the initial room-temperature intensity, with nearly 100% recovery on rewarming. Finer-grained pyrrhotites (but of uncontrolled and imprecisely known submicron sizes) in claystones

exhibit what has been termed the P-transition (Aubourg & Pozzi 2010), a ramp-like and perfectly reversible change in magnetization over the temperature range 50–10 K. This is in contrast to the step-like change in larger pyrrhotite particles over a very narrow temperature range around $T_{Bs}$. The P-transition is quite sensitive to even very weak ambient fields, and may be manifested as an increase or a decrease in magnetization while cooling in the imperfectly controlled zero field ($\pm$500 nT after careful adjustment) of the Quantum Designs Magnetic Property Measurement System (MPMS) instrument commonly used for low-temperature measurements. Depending on the relative abundances of paramagnetic iron-bearing minerals, submicron pyrrhotite and other remanence-bearing phases, the P-transition may be difficult or impossible to discern.

Given the possibility of poorly expressed or entirely suppressed low-temperature transitions in magnetite and pyrrhotite, any definitive quantification of their respective contributions to natural and artificial remanences remains challenging. The large spheroidal particles extracted from a number of remagnetized carbonates (McCabe *et al.* 1983; Suk *et al.* 1990*a*, *b*, 1993; Suk & Halgedahl 1996) have been definitively shown – by x-ray diffraction and scanning electron microscopy (SEM) energy-dispersive analysis – to consist in most cases of nearly pure magnetite. No evidence of magnetic sulphides was found in any of these studies on Appalachian Palaeozoic carbonates, although some grain morphologies such as framboids almost certainly indicate formation of magnetite by replacement of early-diagenetic pyrite (e.g. Reynolds 1990; Suk *et al.* 1990*a*) or perhaps greigite (e.g. Roberts *et al.* 2011). Pyrrhotite has been observed petrographically in carbonates from the lower Carboniferous Leadville Formation of central Colorado that also contain authigenic magnetite (Xu *et al.* 1998). By measuring hysteresis loops of individual extracted spheroidal particles using an extremely sensitive alternating gradient magnetometer, Suk & Halgedahl (1996) made two key additional observations. First, the saturation magnetic moment of many of the spherules was much less than it would be for the same mass of pure magnetite; these must contain large portions of void space, non-magnetic minerals (e.g. silicates or pyrite) and/or weakly magnetic phases such as hematite or goethite. Second, although some relatively large (up to 100 μm) spherules yielded $M_r/M_s$ ratios of 0.5 or more (generally those with quite low $M_s$), the trend for the spherule samples on the Day plot differed strongly from that of the bulk rocks; these can be interpreted as SSD–MD mixtures and SP–SSD mixtures, respectively (Suk & Halgedahl 1996; Dunlop 2002*b*). The bulk rocks contain a large population of ultrafine SP and SSD particles that evade or are destroyed by the extraction process (e.g. Sun & Jackson 1994; Weil & Van der Voo 2002) and whose mineralogy is not constrained by any direct evidence.

## New results

We will now attempt to address some of the outstanding questions described above through the results of experiments conducted on a new sample set collected from Devonian carbonates of the Helderberg Group in New York State (Fig. 3a). These new samples were collected in the Hudson Valley fold-thrust belt just to the north of Kingston, NY at sites along roadcuts on the north side of Route 199 that correspond to two of the localities sampled by Scotese *et al.* (1982) (Fig. 3b, c). Oriented cores were collected from: limestone mudstone with fine-scale laminations of the Manlius Formation (our stratigraphic section H2; site 24 of Scotese *et al.* 1982); limestone packstone comprised predominantly of brachiopod shells with a fine-grained mud matrix of the Becraft Limestone (our stratigraphic section H1 metre levels 0 to 1.4; site 23 of Scotese *et al.* 1982); and from limestone mudstone and wackestone of the Alsen Formation (our stratigraphic section H1 metre levels above 1.4; also site 23 of Scotese *et al.* 1982). The thermal demagnetization of Scotese *et al.* (1982) isolated a characteristic remanence direction from these localities interpreted to be held by magnetite whose direction corresponds with that of other remagnetized Appalachian basin carbonates.

In addition to analyses on these new samples, we also reanalyse some of the earlier datasets (Jackson 1990; Jackson *et al.* 1993) in light of more recent developments in hysteresis loop processing (Fabian 2006; Jackson & Sølheid 2010), with particular attention to the question of undersaturation.

### *Reanalysis of previous hysteresis loops*

The measurements of Jackson (1990) on samples of the Trenton, Onondaga and Knox carbonates used maximum fields of 1 T or less; in some cases 500 mT or even 300 mT was the maximum applied field. With fields of this magnitude it is legitimate to question whether the magnetization was saturated over the region used for high-field slope fitting. Although a few of those samples were archived, most were not, so we cannot remeasure them in higher fields. However, the original loop measurement data are still available and can be reprocessed using statistical tests for non-saturation and non-linear approach-to-saturation fitting (Fabian 2006; Jackson & Sølheid 2010) in the high-field interval.

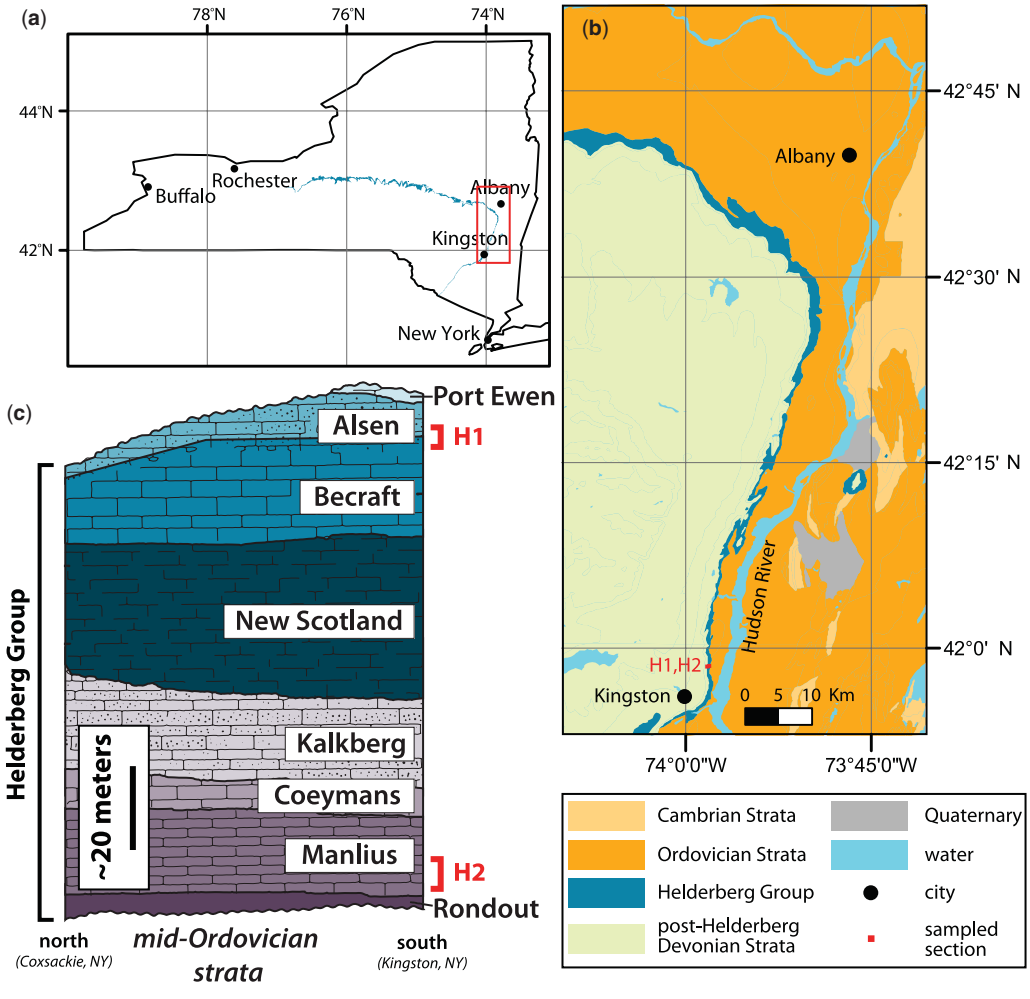


**Fig. 3.** (**a**) Map of New York State with the Helderberg Group mapped out in blue (bedrock geology from Fisher *et al.* 1970). (**b**) Simplified geological map in the vicinity of Kingston and Albany, NY (modified from Fisher *et al.* 1970). The sites sampled in this study to the north of Kingston, New York comprised a stratigraphic section across the contact between the Becraft and Alsen Formations (H1; 41.97604°N, 073.97581°W) and a stratigraphic section within the Manlius Formation (H2; 41.97604°N, 073.97581°W). (**c**) Stratigraphic relationships between the formations that comprise the Helderberg Group between Coxsackie and Kingston, NY above its basal unconformity with the underlying Ordovician flysch of the Austin Glen Formation (modified from Fisher 1987).

The highest $M_r/M_s$ ratios in the original study (in some cases exceeding 0.5) were obtained for the Knox Dolomite and, in a number of cases, these samples were measured in maximum fields of 300 mT under the assumption that this would be sufficient to saturate magnetite. Reprocessing shows that this was far from a safe assumption: F tests (Jackson & Sølheid 2010) comparing total-misfit variance with pure-error variance (quantified by departures from inversion symmetry) indicate that we must reject the hypothesis of linearity over the interval from 70% to 100% of the maximum applied field, with a high degree of certainty (F ranges from 300 to over 1000; compared to a critical value of about 1.5). Recalculation using a non-linear fitting method yields significantly higher estimates of $M_s$ and accordingly diminished estimates of $M_r/M_s$ (Fig. 4). The calculated coercivity is also affected by the slope correction, and both coordinates on the Day plot therefore differ from those originally published by Jackson (1990). This revised analysis undermines the original argument for multiaxial anisotropy that was based on the apparent occurrence of $M_r/M_s$ ratios above 0.5, the theoretical

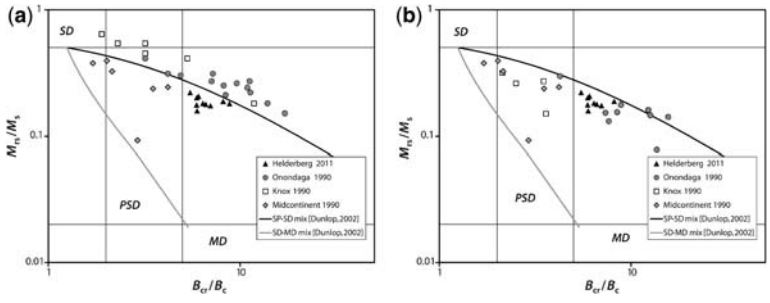


**Fig. 4.** (**a**) Day plot for Onondaga and Knox samples of Jackson (1990), together with new data for mid-continent samples (Jackson *et al.* 1992) and for new Helderberg Group samples. (**b**) Recalculated parameters for the Knox Dolomite and Onondaga Limestone loops, using an approach-to-saturation fit to estimate $M_s$ (see text).

upper limit for uniaxial anisotropy. However, these lowered recalculated $M_r/M_s$ ratios alone do not rule out the possibility of a significant contribution from such particles.

### *Tests for multiaxial anisotropy*

The experimental approach of Lanci's (2010) test for multiaxial anisotropy (Fig. 2) is straightforward, but for instrumental reasons we have modified it slightly. Lanci's technique began with an initial AMS determination followed by pulse magnetizing in 1 T to produce SIRM, and then involved repeated AMS measurements following tumbling AF demagnetization steps to document the gradual removal of the strong field-impressed AMS in multiaxial SD grains. Lacking a tumbling AF instrument, we have slightly modified the experiment for the Helderberg Group samples and have worked in the opposite direction. We begin in the NRM state where moments are very weakly aligned and, after measuring initial AMS, we imprinted an IRM in one or more field steps, remeasuring AMS after each step.

As shown in Table 1, the effect of exposure to strong fields on the AMS of the Helderberg Group samples was negligible. Diagonal tensor elements change by much less than 1%. Because most of the susceptibility comes from paramagnetic and superparamagnetic sources, there is a relatively large correction that must be applied. Consequently there are rather large uncertainties in the corrected degree of anisotropy, but it is nevertheless clear that the AMS of the potential remanence carriers (i.e. the non-SP ferrimagnetic population) is strongly controlled by uniaxial grain-scale anisotropy.

The dominance of uniaxial anisotropy in the analysed Helderberg Group samples is also confirmed in experiments using the approach of Mitra *et al.* (2011) (Fig. 2). These experiments began in the NRM state with no prior exposure to DC or AC fields, and continued with stepwise application of fields of increasing strength ultimately to 1 T. For

**Table 1.** *Field-impressed changes in AMS on Helderberg Group limestones*

| Specimen_ID | $k_{xx}$ | $k_{yy}$ | $k_{zz}$ | Treatment |
|---|---|---|---|---|
| H1-2.3C (Alsen Formation) | 54.25 | 56.09 | 59.73 | None (NRM state) |
| H1-2.3C | 54.37 | 56.28 | 59.81 | 1 T field along $z$ |
| Percent change | 0.22% | 0.34% | 0.13% | |
| H1-2.6B (Alsen Formation) | 147.63 | 154.00 | 156.18 | None (NRM state) |
| H1-2.6B | 147.42 | 154.77 | 156.37 | 100 mT along $x$ |
| Percent change | 0.14% | 0.50% | 0.12% | |
| H1-2.6B | 147.68 | 154.93 | 156.63 | 200 mT along $x$ |
| Percent change | 0.04% | 0.60% | 0.29% | |
| H2-5.35B (Manlius Formation) | 216.98 | 226.28 | 222.78 | None (NRM state) |
| H2-5.35B | 216.59 | 225.94 | 221.99 | 1 T field along $z$ |
| Percent change | 0.18% | 0.15% | 0.35% | |

$k_{xx}$, $k_{yy}$, $k_{zz}$: diagonal elements of susceptibility tensor ($\mu$SI) in the specimen coordinate system

each field step, the field was first applied in the positive direction; the resulting remanence ($M_r^+$) was measured. The same field was then applied in the negative direction and again the resulting remanence ($M_r^-$) was measured. For several samples the experiment was carried out using a pulse magnetizer and a 2G superconducting magnetometer. For a few samples, an equivalent experiment was conducted, using a vibrating-sample magnetometer to measure a series of minor hysteresis loops with increasing peak fields (of equal strength in the positive and negative directions). In all cases, the difference between $M_r^+$ and $M_r^-$ was negligible, thereby demonstrating that the anisotropy of the particles in the analysed Helderberg Group carbonates is overwhelmingly uniaxial (Fig. 5).

### *Superparamagnetic fraction*

Although the SP population plays no role in carrying the NRM, it is of considerable interest in understanding the origins and significance of the (presumably) cogenetic SSD particles that do carry the palaeomagnetic information in these rocks. Further, any quantitative analysis and interpretation of in-field (hysteresis and susceptibility) measurements must properly account for the SP fraction in order to isolate the contribution of the stable remanence carriers.

Magnetic properties change dramatically with increasing size within the SP range and across the SP–SSD threshold (or blocking volume), and are strongly temperature dependent (Néel 1949; Dunlop & Özdemir 1997). SP particles that are much smaller than the blocking volume at a given temperature remain in equilibrium with ambient fields, even those that alternate at high frequency; they therefore have frequency-independent susceptibility that is fully in-phase, and not especially high (e.g. Worm 1998). During hysteresis experiments, these SP particles approach saturation slowly in relatively high fields (Tauxe *et al.* 1996). Larger particles near the SP–SSD threshold show more strongly time- or frequency-dependent magnetization on laboratory measurement timescales; susceptibilities are very high with in-phase ($k'$) and quadrature ($k''$) components that vary with frequency. These 'viscous superparamagnetic' (VSP) particles saturate in relatively low fields, thereby 'shearing' the loop of accompanying stably magnetic phases during hysteresis experiments to generate 'wasp-waisted' loops (Fig. 1b; Tauxe *et al.* 1996; Fabian 2003).

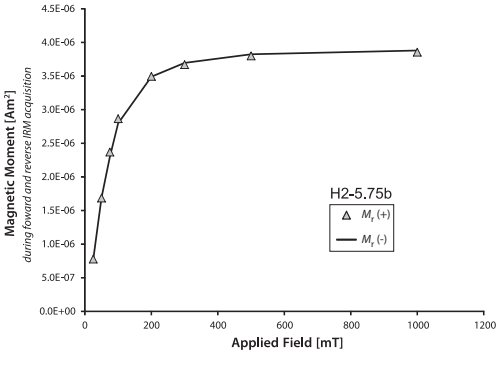


**Fig. 5.** Results of a test for multiaxial anisotropy based on forward and reverse IRM acquisition (Fig. 2; Mitra *et al.* 2011). At each field step a positive field is applied, the resulting remanence ($M_r^+$) is measured, a negative field of equal strength is applied and the remanence ($M_r^-$) is measured. Intensity differences for this sample of the Manlius Formation of the Helderberg Group are negligible, showing that the particle anisotropy is overwhelmingly uniaxial.

At room temperature, a relatively strong (10–20% per decade) frequency dependence of susceptibility and high ratios of $\chi_f/M_s$ (*c.* 50 μm $A^{-1}$) in previously studied remagnetized carbonates (Jackson *et al.* 1993) and in our new Helderberg Group samples clearly indicates the presence of a significant population of grains with $T_b$ *c.* 295 K (for magnetite, this $T_b$ implies grains with diameters of *c.* 15–25 nm; Worm 1998). During cooling, as the size window for VSP behaviour shifts to finer sizes, a strong frequency dependence of $k'$ and a significant $k''$ persist down to 20 K for the Helderberg Group samples (Fig. 6), indicating a broad distribution of nanometric particle sizes.

Hysteresis loops measured on a Quantum Designs MPMS, using maximum fields of 2.5 T and temperatures from 300 K down to 10 K, show strong, progressive increases in $M_r$ and $B_c$ on cooling (Fig. 7) as the SP fraction becomes thermally stable. The loop constriction that is so prominent at room temperature gradually gives way to more 'rectangular' or 'pot-bellied' shapes (Tauxe *et al.* 1996; Fabian 2003). Quantitative loop analysis requires initial separation of the ferrimagnetic signal from the dia/paramagnetic background signal. This becomes somewhat problematic at the lowest temperatures however, where paramagnetic magnetization becomes a distinctly non-linear function of applied field (especially in fields over 1 T). Further, antiferromagnetic nanoparticles of materials such as ferrihydrite may contribute to low-temperature high-field non-linearity. Here we use a consistent fitting method, in which the high-field interval is tested for statistically significant deviations from linearity (Jackson & Sølheid 2010). An exponential approach-to-saturation law (Fabian 2006) is applied if the linearity test fails. We recognize that this method overestimates $M_s$ for the lowest temperatures, because it incorporates some of the non-linear paramagnetic and/or antiferromagnetic magnetization into the modelled ferrimagnetic loop; however

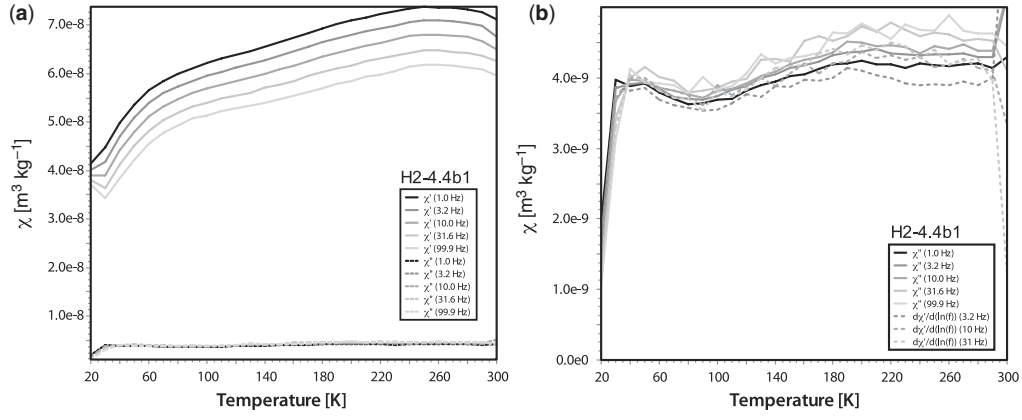


**Fig. 6.** (**a**) In-phase and quadrature susceptibility at five frequencies for sample H2-4.4 (Manlius Formation, Helderberg Group), measured from 20 to 300 K. Strong frequency dependence over the whole temperature range indicates a broad size distribution of nanoparticles (e.g. Worm 1998). (**b**) Expanded view of quadrature susceptibilities, compared to the derivative of in-phase susceptibility with respect to ln($f$).

this will not be critical to our analysis. For temperatures down to about 40 K, $M_s$ changes by only a very slight amount; $M_r$ however increases to 3 times its room-temperature value and $B_c$ increases by a factor of 6 (Figs 8a, b), both as a result of SP–SSD transitions in progressively finer particles on cooling. The shape parameter $\sigma_{hys}$ defined by Fabian (2003) quantifies the dramatic change from strongly wasp-waisted loop shapes to more rectangular or pot-bellied shapes at lower temperatures (Fig. 8c). The sharp increase in calculated $M_s$ values below 40 K is no doubt partly due to the aforementioned non-linear paramagnetic signal affecting the approach-to-saturation calculations, but may also be partly due to ordering of some iron-bearing phase. Jackson & Worm (2001) saw evidence of this ordering in low-temperature susceptibility data for specimens of the Trenton Limestone.

Thermal demagnetization of a low-temperature strong-field isothermal remanence can be used, together with some assumptions, to quantify the SP content in a sample (Banerjee *et al.* 1993) and to calculate the size distribution of particles that unblock while warming to room temperature (e.g. Worm & Jackson 1999). The key assumption is that the loss of remanence is related to the SSD-SP transition, rather than to multi-domain phenomena such as wall unpinning or domain reorganization due to the changes in temperature-dependent anisotropy constants (e.g. Moskowitz *et al.* 1998). This assumption is well justified for the remagnetized carbonates that we are discussing, as detailed

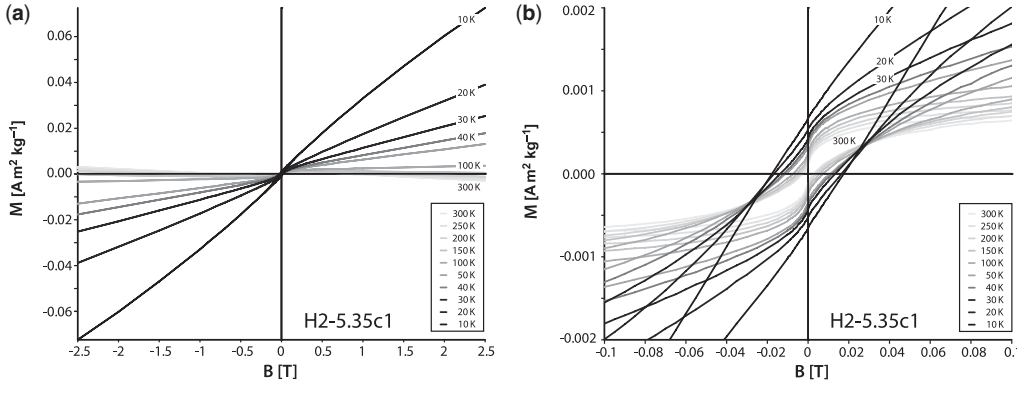


**Fig. 7.** (**a**) Low-temperature high-field hysteresis loops for sample H2-5.35 (Manlius Formation, Helderberg Group), uncorrected for dia- and paramagnetic background. (**b**) Expanded view of low-field portion of the loops, showing the characteristic wasp-waisted shape at room temperature (light grey). This wasp-waisted shape dissipates significantly on cooling as the superparamagnetic particles become progressively blocked in.

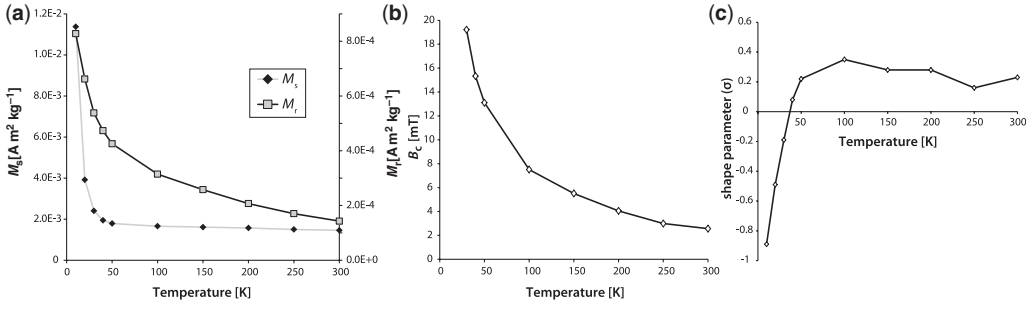


**Fig. 8.** (**a**) Saturation remanence, (**b**) coercivity and (**c**) shape parameter as a function of temperature as calculated for the low-temperature hysteresis loops of sample H2-5.35 (Fig. 7). (a) Saturation remanence increases significantly on cooling, as SP particles become thermally stable. Saturation magnetization changes little, at least down to 40 K, which appears to be the ordering temperature of an unidentified iron-bearing phase. Loop shapes are constricted (positive value of $\sigma$) down to 40 K, below which most of the ferrimagnetic signal comes from thermally stable carriers.

below. For the analysed Helderberg Group samples, roughly three-quarters of the low-temperature remanence imposed isothermally by a 2.5 T field at 20 K is erased by zero-field warming to room temperature. This result implies that approximately 75% of the ferrimagnetic material present is in the SP state at 300 K and does not contribute to the ancient NRM (Fig. 9a). This result agrees well with the estimate of Dunlop (2002*b*) for the Onondaga and Trenton Limestones that was based on modelling of room-temperature hysteresis data. The uninflected demagnetization curve suggests a broad, unimodal size distribution of the SP particles, and simple calculations using the method of Worm & Jackson (1999) make this explicit (Fig. 9b). The distribution peaks at or below $10^{-24}$ m$^3$ (approximately 10 nm diameter), in very good accord with the modelled SSD-SP mixing curves of Dunlop (2002*b*).

## *Stable SD fraction*

Whereas in-field measurements such as hysteresis and susceptibility are strongly influenced by SP particles, we can isolate the properties of the SSD and larger fraction by measuring remanent magnetizations. IRM acquisition and AF demagnetization curves for the new Helderberg Group samples are essentially identical to those obtained previously for the Onondaga and Trenton limestones (Jackson 1990), intersecting at fields of about 50 mT, with crossover parameters (Cisowski 1981) of $R\ c.$ 0.5 (Fig. 10). Roughly 10% of the 1 T SIRM survives AF demagnetization at 200 mT. The acquisition curves strongly resemble those found by Elmore *et al.* (2006) in Helderberg Group samples from West Virginia. They also exhibit some similarity to those defined by unmixing analysis (Gong *et al.* 2009) as the dominant component in remagnetized Cretaceous carbonates from the Organyá Basin of northern Spain, showing significant lack of saturation in 300 mT. Gong *et al.* (2009) interpreted this component as due to very fine magnetite, near the SP–SSD transition. Low-temperature cycling of a room-temperature SIRM (Fig. 11) suggests the presence of minor amounts of remanence-carrying hematite and pyrrhotite, with subtle inflections

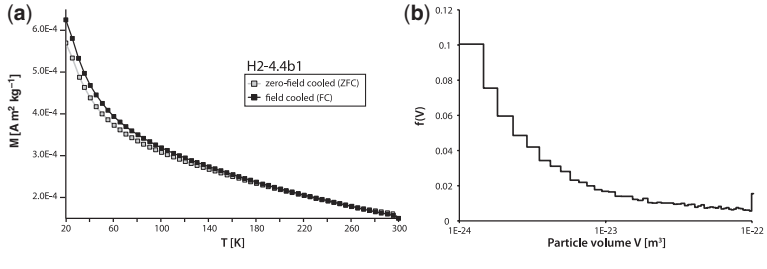


**Fig. 9.** (**a**) Thermal demagnetization of low-temperature remanence for sample H2-4.4 shows progressive unblocking of the nanophase ferrimagnets, with no indication of the Verwey transition. FC remanence was imprinted by cooling in a 2.5 T field from 300 K to 20 K; ZFC remanence was imparted isothermally at 20 K by application and removal of a 2.5 T field (after zero-field cooling from 300 K). Both remanences were measured while warming in zero field. (**b**) Particle-size distribution calculated for the ZFC curve in (a).

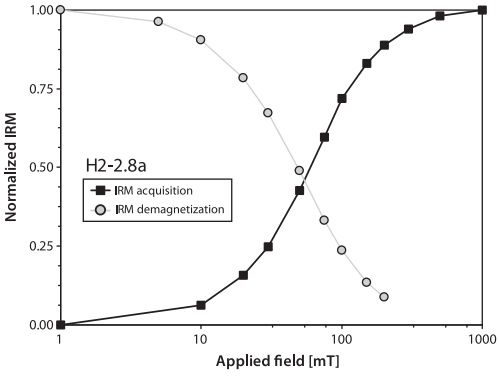


**Fig. 10.** Acquisition and AF demagnetization of IRM for sample H2-2.8 (Manlius Formation, Helderberg Group) shows near-ideal non-interacting SD behaviour (Cisowski 1981). The crossover point between the acquisition and demagnetization curves is 54 mT, $R = 0.46$.

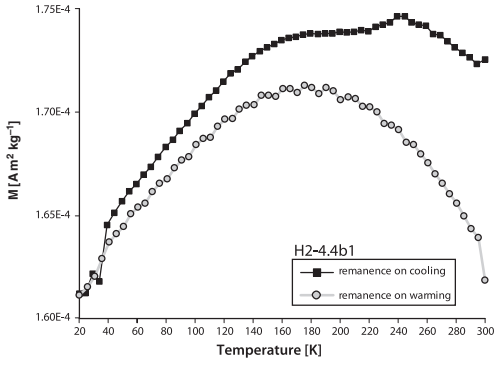


**Fig. 11.** Low-temperature demagnetization (LTD) cycle for H2-4.4. The sample was magnetized isothermally at 300 K in a 2.5 T field, then measured in zero field while cooling to 20 K and rewarming to room temperature. The broad maximum around 150–200 K resembles that observed by Özdemir & Dunlop (2010) in oxidized submicron magnetite; however, here we see no distinct indication of the Verwey transition. The Morin transition (250 K) and the Besnus transition (32 K) indicate small remanence contributions from hematite and pyrrhotite, respectively.

near the Morin transition (*c.* 250 K; e.g. Özdemir & Dunlop 2006) and near the Besnus transition (32 K; Besnus 1966; Dekkers *et al.* 1989; Rochette *et al.* 1990). However, the magnetization changes very little overall (less than 8%) during cooling and rewarming, with some small irreversible loss of remanence. The major feature of the rewarming curve is a broad maximum between 150 and 200 K, resembling the hallmark features noted for oxidized magnetite by Özdemir & Dunlop (2010) and for pyrrhotite by Dekkers (1989).

Anhysteretic remanent magnetization (ARM) acquisition characteristics provide additional evidence that the remanence carriers in many remagnetized carbonate units overwhelmingly comprise non-interacting SSD particles. ARM intensity increases rapidly as a function of DC bias field ($B_{dc}$), with ratios of ARM/SIRM reaching nearly 30% for $B_{dc} = 0.2$ mT (Fig. 12; see also Jackson *et al.* 1992, 1993). The initial slope (calculated for $0 \leq B_{dc} \leq 0.01$ mT) is the normalized anhysteretic susceptibility $\chi_a$/SIRM with a value of 2.1 mm $A^{-1}$, comparable to theoretical values for non-interacting SD magnetite (Egli & Lowrie 2002; Egli 2006), to values observed for cultured magnetotactic bacteria (Moskowitz *et al.* 1993) and for igneous materials such as the Tiva Canyon Tuff (Till *et al.* 2010) and the Lambertville plagioclase (Dunlop & Özdemir 1997, fig. 11.6) that are known to contain dominantly non-interacting SSD magnetic particles.

To summarize, ARM and IRM characteristics together indicate that the thermally stable (non-SP) room-temperature remanence carriers in the new sample set from the Helderberg Group, and from similar previously analysed remagnetized carbonates in the Appalachian Basin and the mid-continental USA, are almost entirely in the SD state with very minimal contributions from PSD and MD grains. These SSD particles are dominated by uniaxial anisotropy and constitute roughly a quarter of the ferrimagnetic material

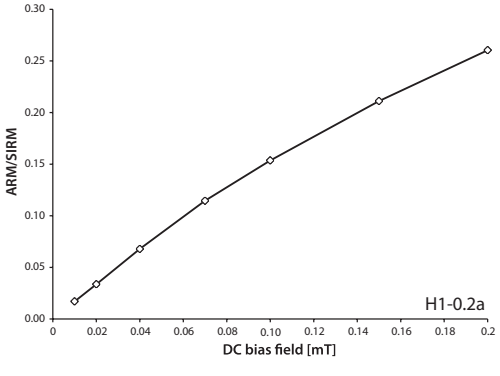


**Fig. 12.** Non-linear anhysteretic remanent magnetization (ARM) acquisition for sample H1-0.2 (Becraft Formation, Helderberg Group) shows non-interacting SD behaviour (Dunlop & Özdemir 1997, fig. 11.8; Egli & Lowrie 2002; Egli 2006). Initial slope gives $\chi_a$/SIRM $= 2.1 \times 10^{-3}$ m $A^{-1}$, comparable to theoretical values for non-interacting SD magnetite (Egli & Lowrie 2002; Egli 2006), to values observed for cultured magnetotactic bacteria (Moskowitz *et al.* 1993) and for igneous materials such as the Tiva Canyon Tuff (Till *et al.* 2010) and the Lambertville plagioclase (Dunlop & Özdemir 1997, fig. 11.6)

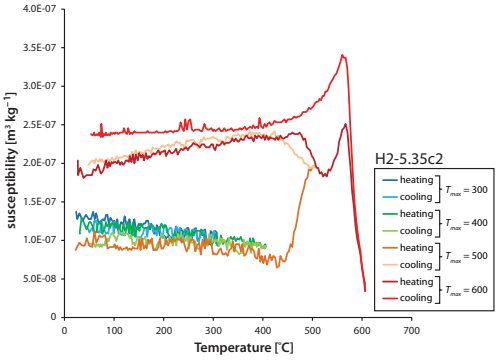


**Fig. 13.** Multicycle high-temperature susceptibility measurements for sample H2-5.35 (Manlius Formation, Helderberg Group) show nearly reversible behaviour below 400 °C (with some decrease due to the 400 degree step), followed by a major increase on heating to 500 °C.

in these samples. Almost all of the rest of the magnetic mineralogy is superparamagnetic at room temperature, as shown by low-temperature hysteresis, low-temperature remanence, frequency-dependent susceptibility and mixing models of room-temperature hysteresis. From these experiments the distribution of domain states is well defined, but specifics of the mineralogy remain elusive.

### *Ferrimagnetic mineral composition*

Given the lack of pronounced diagnostic low-temperature transitions, the best remaining hope for definitive identification of the magnetic mineralogy is through measurements above room temperature. Low-field high-temperature AC susceptibility of the new Helderberg Group samples, measured on a KLY-2 Kappabridge in an argon atmosphere in a series of heating–cooling cycles with successively higher peak temperatures, shows a weak and noisy signal but essentially reversible behaviour up to 400 °C followed by sharp increases in susceptibility for higher-temperature cycles (Fig. 13). This behaviour is virtually identical to that observed by Zegers *et al.* (2003), which they attributed to formation of new magnetite by oxidation of pyrite in the temperature range 420–500 °C. It differs significantly from the results obtained for the Trenton Limestone by Jackson & Worm (2001), in which significant mineral alteration also began for heating runs to maximum temperatures above 400 °C, but the new mineral was most likely pyrrhotite with a Curie temperature near 320 °C.

High-temperature hysteresis measurements (Fig. 14) also had rather marginal signal/noise ratios, due to the combination of weak intensities and small allowable sample sizes. Loops and backfield remanence curves were measured between room temperature and 400 °C, in order to focus on the naturally occurring ferrimagnetic population and avoid the formation of new magnetic material at higher temperatures. Saturation magnetization decreases by about 50% between 20 and 400 °C, significantly more than the drop of *c.* 38% expected for pure magnetite over this temperature interval. This may be due to a small contribution from ferrimagnetic pyrrhotite as a slight dip in the $M_s$(T) curve near 300 °C suggests; however, the data are not of sufficient quality to allow decisive determination. Nevertheless, the trend suggests that monoclinic pyrrhotite is not a major phase in these

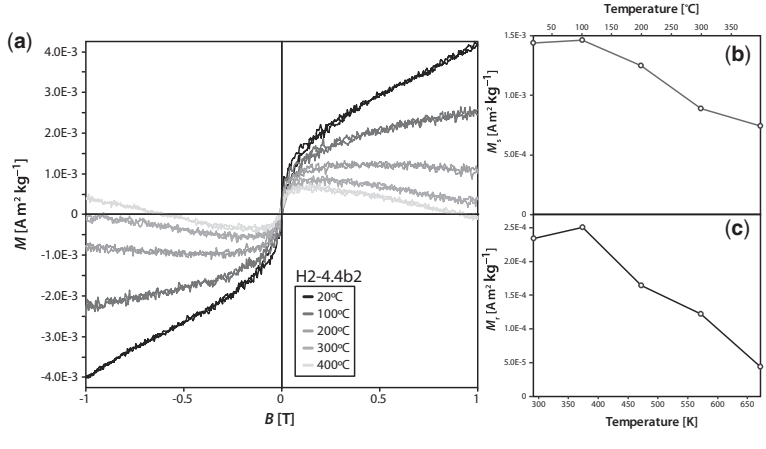


**Fig. 14.** (**a**) High-temperature hysteresis loops for sample H2-4.4, measured on a Princeton Measurements MicroMag VSM (temperatures from 20 to 400 °C). (**b**) Calculated saturation magnetization and (**c**) saturation remanence as functions of temperature.

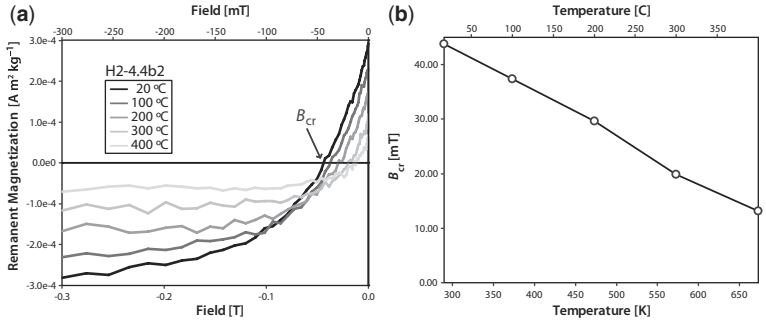


**Fig. 15.** (**a**) High-temperature back-field remanence curves for sample H2-4.4, measured on a Princeton Measurements MicroMag VSM (temperatures from 20 to 400 °C). (**b**) Remanent coercivity determined from the back-field remanence curves as a function of temperature.

samples. Saturation remanence drops by nearly 80% over this temperature range, and the ferrimagnetic population is almost entirely in the SP state by 400 °C. The backfield remanence curves (Fig. 15) show a corresponding progressive shift of the coercivity spectrum to lower fields, with a decrease in $B_{cr}$ by roughly two-thirds over this temperature range.

The method of Lowrie (1990) for identifying remanence carriers according to both coercivity and unblocking-temperature ranges yields similar results (Fig. 16). Orthogonal IRMs were imprinted with successively decreasing pulsed fields: 1 T along the specimen $z$ axis, 300 mT along $x$ and 100 mT along $y$. The two lower-field treatments each reoriented most of the remanence acquired in previous steps (Fig. 16a), confirming that hard antiferromagnets such as hematite could only be making a minor contribution to the IRM. Stepwise thermal demagnetization shows that the three coercivity fractions all unblock at approximately the same rate, with more than 80% of the remanence erased by 400 °C and nearly 100% demagnetized by 500° (Fig. 16b). A slight change in slope in the intermediate-coercivity $x$ component from 300 to 350 °C may be due to pyrrhotite, but overall the remanence appears to reside in a magnetite-like phase with relatively low unblocking temperatures.

The low-temperature data clearly show that stoichiometric magnetite is nearly absent from these samples. Cation-deficient magnetite is a good candidate to account for the low-T properties, but is less successful in accounting for $M_s$(T) above room temperature since oxidation increases the Curie temperature (Özdemir & Banerjee 1984). The observed $M_s$(T) trend suggests a Curie temperature below that of pure magnetite. Cation substitution could account for this, but would be quite surprising as it would seem to be inconsistent with a low-temperature chemical origin for the

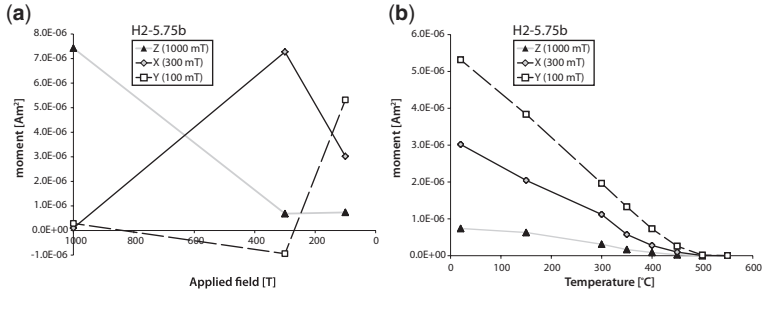


**Fig. 16.** (**a**) Acquisition and (**b**) thermal demagnetization of a three-component IRM for sample H2-5.75 (Manlius Formation, Helderberg Group). Acquisition involved application of a 1 T pulsed field along the specimen's $z$ axis, followed by a 300 mT field along the $x$ axis and a 100 mT field along the $y$ axis. The two latter treatments each reorient most of the remanence, thus shown to be carried predominantly by relatively soft (ferrimagnetic) phases. The three components are removed at roughly the same rates by thermal demagnetization, and are almost completely removed by 500 °C. A dip in the intermediate-coercivity $x$ component at 300–350 °C may be due to pyrrhotite.

dominant magnetic phase. On the other hand, Xu *et al.* (1998) found magnetite grains of clearly authigenic origin that contained minor amounts of substituted Ti and Mn ($x < 0.15$ in $Fe_{3-x}Ti_xO_4$) in the Leadville carbonates of central Colorado. Such compositions would suppress the Verwey transition and also depress the Curie temperature and unblocking temperatures. However, authigenic cation-substituted magnetite has not (to our knowledge) been found in other studies of remagnetized carbonates. Probably the best way to explain both the low- and high-temperature data is through a mixture of maghematized magnetite and smaller amounts of monoclinic pyrrhotite nanoparticles, but cation-substituted authigenic magnetite may also be important.

## Discussion

Do hysteresis properties provide reliable indications of the presence or absence of substantial chemical overprints in carbonate rocks? Certainly *in situ* growth of a significant population of SP–SSD particles should be expected to exert a strong influence on both the NRM and on the rock-magnetic properties, and a number of studies have confirmed this relationship. But how often might we encounter 'false positives' (hysteresis ratios along the trend defined by the remagnetized Appalachian basin carbonates, in rocks where the characteristic remanence is primary) or 'false negatives' (hysteresis ratios along the trend for SD–MD magnetites, in rocks that are substantially or completely remagnetized)? How might we recognize these situations? Given the variety of possible remagnetization mechanisms and triggers (e.g. Elmore 2001), as well as the variety of possible primary iron phases in carbonates, there are a number of important points that have to be considered.

### *Primary magnetic particles in carbonates: sources, characteristics, preservation*

Major proportions of SP material are relatively rare in geological materials, with notable exceptions mostly including those in which the SP material formed *in situ*: soils and palaeosols (e.g. Mullins 1977; Maher & Taylor 1988; Dearing *et al.* 1997; Guyodo *et al.* 2006); rapidly cooled volcanics (e.g. Schlinger *et al.* 1991; Gee & Kent 1999; Till *et al.* 2010); and marine or lacustrine sediments where SP magnetite is produced in the sediment column by dissimilatory iron-reducing bacteria (e.g. Moskowitz *et al.* 1989; Maloof *et al.* 2007). The high surface area to volume ratios of SP magnetite likely contribute to their geochemical instability in detrital environments (e.g. Li *et al.* 2009). Carbonates with primary magnetization from which hysteresis data have been obtained reveal a trend on the compiled Day plot of hysteresis parameters (Fig. 1) that indicates magnetite populations dominated by SD and MD particles without significant SP contributions. These units are predominantly deepwater pelagic limestones (Laytonville Limestone, Maiolica Limestone, ODP 728) and, in such lithologies, an SD–MD grain size distribution is consistent with detrital input of magnetite and either a lack of SP input or alteration of any SP particles. However, in shallow-water carbonate depositional environments that are isolated from aqueous detrital input and where there is early cementation, is it possible that there could be significant contributions of both ultrafine SP and SSD ferrimagnets? If so, they may yield false positive indications of remagnetization. In the absence of aqueous detrital input there are two main potential sources of magnetic minerals to carbonate environments: biogenic precipitation and aeolian delivery (including extraterrestrial fluxes).

Freeman (1986) documented the common occurrence of 'cosmic spherules' in magnetic extracts from pelagic limestones by detailed SEM work, but was unable to quantify the proportions of ultrafine material in these extraterrestrial magnetic particles. It is not uncommon for airborne dust collections to show significant populations of SP–SSD ferrimagnets, especially when no major local dust sources are present (e.g. Oldfield *et al.* 1985). Magnetic material found in dust layers in the Greenland and Antarctic ice cores contained significant proportions of SP–SSD nanoparticles whose origins were ascribed to ablation of meteorites in Earth's upper atmosphere (Lanci & Kent 2006; Lanci *et al.* 2007, 2008). Detrital inputs of ferrimagnetic nanoparticles could therefore potentially mimic the hysteresis properities of the SP–SSD grains that are produced through authigenic processes associated with remagnetization.

Extracellular formation of magnetite during microbial iron reduction can lead to the *in situ* formation of prodigious amounts of SP magnetite during deposition (Frankel 1987; Maloof *et al.* 2007). Combined with SD grains formed by magnetotactic bacteria during or immediately following deposition (e.g. Kopp & Kirschvink 2008; Moskowitz *et al.* 2008), these populations could also give false indications of remagnetization based on hysteresis properties. With the current published datasets predominantly coming from deepwater carbonates, the possibility that there can be preservation of a significant primary SP population in early cemented shallow-water carbonates is difficult to evaluate. This reality points to the need for more detailed hysteresis data from shallow-water carbonates to see if the preservation of primary SP grains can have a significant influence on hysteresis parameters.

Primary detrital magnetic oxide grains in the PSD and MD size range can moreover be diminished to SP–SSD sizes by reductive dissolution (e.g. Karlin & Levi 1983; Tarduno 1995; Smirnov & Tarduno 2001). New iron sulphide minerals (predominantly greigite) commonly also form in the sediment column during early diagenetic sulphate reduction (Maloof *et al.* 2007; Roberts *et al.* 2011). The combination of such sulphides with residual magnetite could conceivably mimic the hysteresis signature of the remagnetized carbonates, whether or not the new sulphides carry a significant portion of the remanence.

It has long been known that constricted ('wasp-waisted') hysteresis loops and high coercivity ratios can arise from mixtures of hard (e.g. imperfect antiferromagnets such as hematite and goethite) and soft (e.g. ferrimagnets such as magnetite and maghemite) phases (e.g. Nagata & Carleton 1987). There are many situations imaginable (e.g. detrital magnetite and late weathering products such as goethite) where Day plot locations and constricted loops might incorrectly suggest an ancient remagnetization. In the case of a mix of soft ferrimagnetic and hard antiferromagnetic carriers, values of $B_c$ and $B_{cr}$ would be higher than in the case of a dominant SP–SSD population. Additionally, if the loop constriction is due to multiple mineralogies there may be discernible inflections in the gradient of magnetization acquisition and backfield demagnetization of an SIRM. Given the common occurrence of goethite as a surface weathering product and the precipitation of secondary iron sulphides through fluid flow or early diagenesis, interpretations of hysteresis loop parameters should be made cautiously and be paired with other rock magnetic experiments that can demonstrate a largely mono-mineralic population of ferrimagnetic grains.

## *Sources of iron for formation of new magnetic phases and mechanisms and triggers for authigenic iron oxide growth*

Oxidation of pyrite or other sulphides to magnetite in remagnetized carbonates has been documented through detailed analytical microscopy (e.g. Fruit *et al.* 1995; Weil & Van der Voo 2002). Early diagenetic pyrite framboids, aggregates up to 100 μm in diameter comprised of large numbers of small (<1 μm) crystallites, have frequently been found in North American Palaeozoic carbonates to be completely altered by later diagenesis to magnetite (Suk *et al.* 1990*a*, *b*, 1991, 1993). Suk & Halgedahl (1996) found a variety of other iron-oxide spheroid morphologies that may have formed in this way or by different processes (Freeman 1986), many of which exhibited the MD magnetic behaviour expected for particles of that size but some of which had PSD or SSD hysteresis properties; a few even had wasp-waisted loops. They argued that despite the large particle dimensions, such spheroids may be the major remanence carriers in the remagnetized carbonates of the Appalachian Basin and elsewhere. This argument is difficult to refute, especially if we recognize that the spheroid population recovered by magnetic extraction from the insoluble residue is likely to be strongly biased in favour of the larger and more highly magnetic particles, and that therefore the spherules found with relatively low $M_s$ (and high $M_r/M_s$) may be the most representative of those in the bulk rock. However, it is not clear that the preponderance of SP magnetite in bulk-rock remagnetized carbonate samples has any direct association with pre-existing sulphides or with the observed spheroids. Replacement of iron sulphides by magnetite is certainly involved in many cases and may be a chief mechanism of remagnetization when large-scale fluid flow is involved. It remains difficult to predict with any certainty that a distinctive hysteresis signature must necessarily accompany this process, so the possibility of false negative tests cannot be ruled out. Suk & Halgedahl (1996) found 'normal' unconstricted hysteresis loops in remagnetized Onondaga Limestone samples from western New York, suggesting that SP magnetite was not formed by the remagnetization process or not preserved.

Many studies have convincingly demonstrated a connection between remagnetization and clay diagenesis, particularly the conversion of smectite to illite (Jackson *et al.* 1988; Hirt *et al.* 1993; Katz *et al.* 1998; Elliott *et al.* 2006*a*, *b*; Tohver *et al.* 2008). Illitization of smectite occurs at relatively low temperatures (between *c.* 60 °C and 120 °C) and liberates both water and cations such as iron, creating conditions suitable for the *de novo* formation of magnetite or other remanence-carrying minerals. Nucleation and growth processes can be expected to produce nanoparticle populations with size distributions that are ultimately governed by factors including element availability, diffusion rates, reactivity, temperature and time. The growth of magnetite through this process is likely to produce populations that span the SP–SSD size range. In such a scenario, the formation of both abundant SP grains and the grains that reached the critical size for thermal stability (and thus acquisition of a secondary remanence) can be attributed to a single chemical overprinting event. This process seems to us to be the situation in which unique hysteresis properties may most reliably indicate strong chemical remagnetizations analogous to those seen in North American Palaeozoic carbonates.

### *The rock-magnetic signature of remagnetization in carbonate rocks*

Given the wide variety of possible remagnetization mechanisms, parent phases and final carriers, and the range of scenarios discussed above for potential false positives and false negatives, it is somewhat surprising that a rock-magnetic signature of remagnetization would have any generality. This is even more true now that we have eliminated one of the proposed rationales for a distinctive hysteresis signature, based on multiaxial individual-particle anisotropy in equidimensional authigenic magnetites. However, many examples are now available for which demonstrably remagnetized units have some or all of the putative rock-magnetic fingerprints (e.g. Channell & McCabe 1994; McCabe & Channell 1994; Molina Garza & Zijderveld 1996; Suk & Halgedahl 1996; Banerjee *et al.* 1997; Butler *et al.* 1997; Xu *et al.* 1998; d'Agrella Filho *et al.* 2000; Dinares-Turell & Garcia-Senz 2000; Enkin *et al.* 2000; Zegers *et al.* 2003; Trindade *et al.* 2004; Zwing *et al.* 2005; Elmore *et al.* 2006; Soto *et al.* 2008). We are not aware of any clear-cut false positives (hysteresis characteristics indicating complete remagnetization in carbonate rocks bearing a primary NRM) and very few false negatives (hysteresis behaviour indicating primary NRM carriers in fully chemically overprinted carbonate rocks). However, there is a number of rock units with 'intermediate' or ambiguous hysteresis characteristics, some of which clearly have multi-mineralic remanence-carrying populations (e.g. Weil & Van der Voo 2002; Zegers *et al.* 2003; Zwing *et al.* 2005; Oliva-Urcia & Pueyo 2007).

Zwing *et al.* (2005) noted a strong association of lithology and hysteresis properties of remagnetized rocks: reef carbonates, with low primary detrital content, exhibited hysteresis properties similar to those of the archetypal remagnetized carbonates; platform carbonate samples had intermediate hysteresis ratios; and remagnetized siliciclastics had hysteresis properties suggestive of primary detrital mineralogy. They reached the reasonable conclusion that a remagnetization test based on hysteresis behaviour only works when authigenic phases represent an overwhelming majority of the magnetic mineralogy, which in most cases means that detrital phases cannot be present in any great abundance. Indeed, our compilation in Figure 1 also appears to show a systematic dependence on depositional environment, with samples that plot along the 'primary' SD–MD mixing line coming largely from pelagic limestones (Channell & McCabe 1994; Tarduno & Myers 1994; Abrajevitch & Kodama 2009) while the Pleistocene Tahiti reef (Ménabréaz *et al.* 2010) had significant input of volcaniclastic sands. In each of these cases, it appears magnetite from a detrital or bacterial source is holding a primary remanence.

In our view, the most diagnostic indicator of magnetite authigenesis in carbonate rocks is the occurrence of a unimodal particle-size distribution that peaks well below the room-temperature SP–SSD threshold. Such distributions are relatively rare in geological materials and, when they do occur, are almost always associated with *in situ* processes of origin (nucleation and growth in volcanic glass, metabolic electron-transfer reactions mediated extracellularly by bacteria, pedogenesis or various candidate processes in carbonate rocks). Particles that grow through the SP–SSD threshold acquire a stable CRM, and the population characteristics account for the distinctive hysteresis behaviour, high ARM/SIRM ratios and elevated frequency-dependence of susceptibility. Further work is needed, however, to evaluate whether a similar particle-size distribution could arise in the primary magnetic mineralogy of shallow-water carbonates that are isolated from detrital input.

## Summary and conclusions

In the prototypical remagnetized carbonates that have been the principal focus of this study, both the ChRM and the rock-magnetic properties are intimately related to the SP–SSD nanoparticle population that formed *in situ* during the Permian, many tens of millions of years after the strata were deposited. Clay diagenesis and maturation of organic matter, driven by moderately elevated burial temperatures as well as changes in geochemical conditions possibly due to introduction of tectonically driven brines, resulted in neoformation of these nanoparticles and alteration of pre-existing iron sulphides. Large proportions of the authigenic magnetite never grew to sizes larger than 20 nm; these SP particles are responsible for the frequency-dependent susceptibility and, to a large extent, for the wasp-waisted hysteresis loops and strongly elevated $H_{cr}/H_c$ ratios that constitute the proposed rock-magnetic fingerprint of remagnetization. Some fraction of the authigenic magnetite grew through the SP–SSD threshold, acquiring the ChRM and accounting for the elevated ARM/SIRM ratios that help to identify the carriers as authigenic. In the Helderberg Group samples of this study, some 75% of the magnetite is superparamagnetic at room temperature, and almost all of the rest is SSD. The exact mineralogical composition remains unclear, but it is certainly not pure magnetite; some small degree of cation substitution or a larger degree of cation deficiency is required for the almost complete lack of a Verwey transition.

One of the original explanations offered for a correlation between hysteresis properties and strong chemical remagnetization involved authigenic SD particles having an almost complete lack of shape anisotropy (i.e. spheroidal morphologies resembling those observed in large extracted magnetite particles), and therefore having magnetic properties governed primarily by the cubic magnetocrystalline (multiaxial) anisotropy of magnetite (Jackson 1990). We have now shown unequivocally that this is not correct for the newly analysed samples of the Helderberg Group. Two new approaches (Lanci 2010; Mitra *et al.* 2011) applied to these samples to test for the presence of multiaxial anisotropy have revealed that the magnetite particles are instead controlled by uniaxial anisotropy. The fundamental basis of the distinctive hysteresis behaviour of these remagnetized carbonates is the dominant contribution from the SP and SSD size fractions.

It should be borne in mind that although there is a strong link between rock-magnetic behaviour and size distributions in these rocks, the link between particle sizes and a late authigenic origin is more indirect. It is conceivable that dominant SP–SSD size fractions could also originate biogenically or by detrital input, and that rocks with a primary or very early ChRM may therefore sometimes exhibit the rock-magnetic characteristics associated with remagnetization. At this time, we are unaware of any such 'false positives' in the published literature where carbonates with primary magnetization yield hysteresis parameters in the range typically restricted to remagnetized carbonates. Nevertheless, there is a paucity of hysteresis data from shallow-water carbonates with primary ChRMs, and data are needed from such units to further evaluate whether the primary coexistence of SP and SSD grains ever leads to false positives for remagnetization. 'False negative' results (in which remagnetized units have the rock-magnetic characteristic of unremagnetized carbonates) appear to be more common, when detrital materials occur in sufficient abundance to shift the peak of the size distribution into the PSD–MD range.

We thank A. Hirt and an anonymous reviewer for their helpful suggestions and S. Swanson-Hysell for assistance with fieldwork. This is contribution 1106 of the Institute for Rock Magnetism, which is supported by grants from the Instruments and Facilities Program, Division of Earth Science, National Science Foundation.

## References

Abrajevitch, A. & Kodama, K. 2009. Biochemical v. detrital mechanism of remanence acquisition in marine carbonates: A lesson from the K-T boundary interval. *Earth and Planetary Science Letters*, **286**, 269–277.

Aubourg, C. & Pozzi, J. P. 2010. Toward a new <250 °C pyrrhotite-magnetite geothermometer for claystones <250 °C pyrrhotite-magnetite geothermometer for claystones. *Earth and Planetary Science Letters*, **294**, 47–57.

Bachtadse, V., Van der Voo, R., Hayes, F. M. & Kesler, S. E. 1987. Late Paleozoic remagnetization of mineralized and unmineralized Ordovician carbonates from east Tennessee: evidence for a post-ore chemical event. *Journal of Geophysical Research B: Solid Earth*, **92**, 14 165–14 176.

Banerjee, S. K., Hunt, C. P. & Liu, X.-M. 1993. Separation of local signals from the regional paleomonsoon record of the Chinese loess plateau: a rock-magnetic approach. *Geophysical Research Letters*, **20**, 843–846.

Banerjee, S., Elmore, R. D. & Engel, M. H. 1997. Chemical remagnetization and burial diagenesis: testing the hypothesis in the Pennsylvanian Belden Formation, Colorado. *Journal of Geophysical Research*, **102**, 24 825–24 842.

Belkaaloul, N. K. & Aissaoui, D. M. 1997. Nature and origin of magnetic minerals within the Middle Jurassic shallow-water carbonate rocks of the Paris Basin, France: implications for magnetostratigraphic dating. *Geophysical Journal International*, **130**, 411–421.

Besnus, M. J. 1966. *Propriétés magnétiques de la pyrrhotite naturelle*. PhD thesis, University of Strasbourg.

Bethke, C. M. & Marshak, S. 1990. Brine migrations across North America: the plate tectonics of groundwater. *Annual Reviews of Earth and Planetary Sciences*, **18**, 287–315.

Blumstein, A. M., Elmore, R. D., Engel, M. H., Elliot, C. & Basu, A. 2004. Paleomagnetic dating of burial diagenesis in Mississippian carbonates, Utah. *Journal of Geophysical Research*, **109**, 1–16.

Butler, R. F., Gehrels, G. E. & Bazard, D. R. 1997. Paleomagnetism of Paleozoic strata of the Alexander terrane, southeastern Alaska. *GSA Bulletin*, **109**, 1372–1388.

Channell, J. E. T. & McCabe, C. 1994. Comparison of magnetic hysteresis parameters of unremagnetized and remagnetized limestones. *Journal of Geophysical Research B: Solid Earth*, **99**, 4613–4623.

Cisowski, S. 1981. Interacting v. non-interacting single-domain behavior in natural and synthetic samples. *Physics of the Earth and Planetary Interiors*, **26**, 77–83.

D'Agrella Filho, M. S., Babinski, M., Trindade, R. I. F., van Schmus, W. R. & Ernesto, M. 2000. Simultaneous remagnetization and U–Pb isotope resetting in Neoproterozoic carbonates of the Sao Francisco Craton, Brazil. *Precambrian Research*, **99**, 179–196.

Day, R., Fuller, M. & Schmidt, V. A. 1977. Hysteresis properties of titanomagnetites: grain-size and compositional dependence. *Physics of the Earth and Planetary Interiors*, **13**, 260–266.

Dearing, J. A., Bird, P. M., Dann, R. J. L. & Benjamin, S. F. 1997. Secondary ferrimagnetic minerals in Welsh soils: a comparison of mineral magnetic detection

methods and implications for mineral formation. *Geophysical Journal International*, **130**, 727–736.

DEKKERS, M. J. 1989. Magnetic properties of natural pyrrhotite. II. High- and low-temperature behavior of Jrs and TRM as a function of grain size. *Physics of the Earth and Planetary Interiors*, **57**, 266–283.

DEKKERS, M. J., MATTÉI, J.-L., FILLION, G. & ROCHETTE, P. 1989. Grain-size dependence of the magnetic behavior of pyrrhotite during its low-temperature transition at 34 K. *Geophysical Research Letters*, **16**, 855–858.

DINARES-TURELL, J. & GARCIA-SENZ, J. 2000. Remagnetization of Lower Cretaceous limestones from the southern Pyrenees and relation to the Iberian plate geodynamic evolution. *Journal of Geophysical Research*, **105**, 19 405–19 418.

DUNLOP, D. J. 2002*a*. Theory and application of the Day plot (Mrs/Ms v. Hcr/Hc). 1. Theoretical curves and tests using titanomagnetite data. *Journal of Geophysical Research*, **107**, doi:10.1029/2001JB000487.

DUNLOP, D. J. 2002*b*. Theory and application of the Day plot (Mrs/Ms v. Hcr/Hc). 2. Application to data for rocks, sediments, and soils. *Journal of Geophysical Research*, **107**, 1. doi:10.1029/2001JB000486.

DUNLOP, D. J. & ÖZDEMIR, Ö. 1997. *Rock Magnetism. Fundamentals and Frontiers*. Cambridge University Press, Cambridge.

DUNLOP, D. J., ÖZDEMIR, Ö. & SCHMIDT, P. W. 1997*a*. Paleomagnetism and paleothermometry of the Sydney Basin. 2. Origin of anomalously high unblocking temperatures. *Journal of Geophysical Research*, **102**, 27285–27295.

DUNLOP, D. J., SCHMIDT, P. W., OZDEMIR, O. & CLARK, D. A. 1997*b*. Paleomagnetism and paleothermometry of the Sydney Basin. 1. Thermoviscous and chemical overprinting of the Milton Monzonite. *Journal of Geophysical Research*, **102**, 27271–27283.

EGLI, R. 2006. Theoretical considerations on the anhysteretic remanent magnetization of interacting particles with uniaxial anisotropy. *Journal of Geophysical Research B. Solid Earth*, **111**, doi:10.1029/2006JB004577.

EGLI, R. & LOWRIE, W. 2002. Anhysteretic remanent magnetization of fine magnetic particles. *Journal of Geophysical Research-Solid Earth*, **107**, 2209, doi:10.1029/2001JB000671.

ELLIOTT, W. C., BASU, A., WAMPLER, J. M., ELMORE, R. D. & GRATHOFF, G. H. 2006*a*. Comparison of K-Ar ages of diagenetic illite-smectite to the age of a chemical remanent magnetization (CRM): an example from the Isle of Skye, Scotland. *Clays and Clay Minerals*, **54**, 314–323.

ELLIOTT, W. C., OSBORN, S. G., O'BRIEN, V. J., ELMORE, R. D., ENGEL, M. H. & WAMPLER, J. M. 2006*b*. On the timing and causes of illite formation and remagnetization in the Cretaceous Marias River Shale, Disturbed Belt, Montana. *Journal of Geochemical Exploration*, **89**, 92–95.

ELMORE, R. D. 2001. A review of palaeomagnetic data on the timing and origin of multiple fluid-flow events in the Arbuckle Mountains, southern Oklahoma. *Petroleum Geoscience*, **7**, 223–229.

ELMORE, R. D. & MCCABE, C. 1991. The occurrence and origin of remagnetization in the sedimentary rocks of North America. *Reviews of Geophysics*, **29** (Suppl.), 377–383.

ELMORE, R. D., LONDON, D., BAGLEY, D., FRUIT, D. & GAO, G. 1993. Remagnetization by basinal fluids: testing the hypothesis in the Viola Limestone, southern Oklahoma. *Journal of Geophysical Research B, Solid Earth*, **98**, 6237–6254.

ELMORE, R. D., FOUCHER, J. L. E., EVANS, M., LEWCHUK, M. & COX, E. 2006. Remagnetization of the Tonoloway Formation and the Helderberg Group in the Central Appalachians: testing the origin of syntilting magnetizations. *Geophysical Journal International*, **166**, 1062–1076.

ENKIN, R. J., OSADETZ, K. G., BAKER, J. & KISILEVSKY, D. 2000. Orogenic remagnetizations in the Front Ranges and Inner Foothills of the southern Canadian Cordillera: Chemical harbinger and thermal handmaiden of Cordilleran deformation. *Geological Society of America Bulletin*, **112**, 929–942.

EVERITT, C. W. F. & CLEGG, J. A. 1962. A field test of palaeomagnetic stability. *Geophysical Journal of the Royal Astronomical Society*, **6**, 312–319.

FABIAN, K. 2003. Some additional parameters to estimate domain state from isothermal magnetization measurements. *Earth and Planetary Science Letters*, **213**, 337–345.

FABIAN, K. 2006. Approach to saturation analysis of hysteresis measurements in rock magnetism and evidence for stress dominated magnetic anisotropy in young mid-ocean ridge basalt. *Physics of the Earth and Planetary Interiors*, **154**, 299–307.

FISHER, D. W. 1987. Lower Devonian limestone, Helderberg Escarpment. *In*: ROY, D. C. (ed.) *Geological Society of America Centennial Field Guide – Northeastern Section*. Geological Society of America, Boulder, 119–122.

FISHER, D. W., ISACHSEN, Y. W. & RICKARD, L. V. 1970. Geologic Map of New York State (1:250000) New York State Museum Map and Chart Series No. 15.

FRANKEL, R. B. 1987. Anaerobes pumping iron. *Nature*, **330**, 208.

FREEMAN, R. 1986. Magnetic mineralogy of pelagic limestones. *Geophysical Journal of the Royal Astronomical Society*, **85**, 433–452.

FRUIT, D., ELMORE, R. D. & HALGEDAHL, S. 1995. Remagnetization of the folded Belden formation, northwest Colorado. *Journal of Geophysical Research B: Solid Earth*, **100**, 15009–15024.

GARVEN, G. 1995. Continental-scale groundwater flow and geological processes. *Annual Review of Earth and Planetary Sciences*, **24**, 89–117.

GEE, J. & KENT, D. V. 1995. Magnetic hysteresis in young mid-ocean ridge basalts: dominant cubic anisotropy? *Geophysical Research Letters*, **22**, 551–554.

GEE, J. & KENT, D. V. 1999. Calibration of magnetic granulometric trends in oceanic basalts. *Earth and Planetary Science Letters*, **170**, 377–390.

GONG, Z., DEKKERS, M. J., HESLOP, D. & MULLENDER, T. A. T. 2009. End-member modelling of isothermal remanent magnetization (IRM) acquisition curves: a novel approach to diagnose remagnetization. *Geophysical Journal International*, **178**, 693–701.

GOREE, W. S. & FULLER, M. D. 1976. Magnetometers using r-f driven SQUIDs and their application in rock

magnetism and paleomagnetism. *Reviews of Geophysics and Space Physics*, **14**, 591–608.

GRAHAM, J. W. 1949. The stability and significance of magnetism in sedimentary rocks. *Journal of Geophysical Research*, **54**, 131–167.

GUYODO, Y., LAPARA, T. M., ANSCHUTZ, A. J., PENN, R. L., BANERJEE, S. K., GEISS, C. E. & ZANNER, W. 2006. Rock magnetic, chemical and bacterial community analysis of a modern soil from Nebraska. *Earth and Planetary Science Letters*, **251**, 168–178.

HIRT, A. M., BANIN, A. & GEHRING, A. U. 1993. Thermal generation of ferromagnetic minerals from iron-enriched smectites. *Geophysical Journal International*, **115**, 1161–1168.

JACKSON, M. J. 1990. Diagenetic sources of stable remanence in remagnetized Paleozoic cratonic carbonates: a rock magnetic study. *Journal of Geophysical Research B: Solid Earth*, **95**, 2753–2761.

JACKSON, M. J. & WORM, H.-U. 2001. Anomalous unblocking temperatures, viscosity and frequency-dependent susceptibility in the chemically-remagnetized Trenton Limestone. *Physics of the Earth and Planetary Interiors*, **126**, 27–42.

JACKSON, M. J. & SØLHEID, P. 2010. On the quantitative analysis and evaluation of magnetic hysteresis data, Geochemistry, Geophysics. *Geosystems*, **11**, doi:10.1029/2009GC002932.

JACKSON, M. J., MCCABE, C., BALLARD, M. M. & VAN DER VOO, R. 1988. Magnetite authigenesis and diagenetic paleotemperatures across the northern Appalachian Basin. *Geology*, **16**, 592–595.

JACKSON, M. J., WORM, H.-U. & BANERJEE, S. K. 1990. Fourier analysis of digital hysteresis data: rock magnetic applications. *Physics of the Earth and Planetary Interiors*, **65**, 78–87.

JACKSON, M. J., SUN, W.-W. & CRADDOCK, J. P. 1992. The rock magnetic fingerprint of chemical remagnetization in midcontinental Paleozoic carbonates. *Geophysical Research Letters*, **19**, 781–784.

JACKSON, M. J., ROCHETTE, P., FILLION, G., BANERJEE, S. K. & MARVIN, J. A. 1993. Rock magnetism of remagnetized Paleozoic carbonates: low-temperature behavior and susceptibility characteristics. *Journal of Geophysical Research B: Solid Earth*, **98**, 6217–6225.

KARLIN, R. & LEVI, S. 1983. Diagenesis of magnetic minerals in recent haemipelagic sediments. *Nature*, **303**, 327–330.

KATZ, B., ELMORE, R. D. & ENGEL, M. H. 1998. Authigenesis of magnetite in organic-rich sediment next to a dike: implications for thermoviscous and chemical remagnetizations. *Earth and Planetary Science Letters*, **163**, 221–234.

KATZ, B., ELMORE, R., COGOINI, M., ENGEL, M. & FERRY, S. 2000. Associations between burial diagenesis of smectite, chemical remagnetization, and magnetite authigenesis in the Vocontian trough, SE France. *Journal of Geophysical Research*, **105**, 1.

KENT, D. V. 1979. Paleomagnetism of the Devonian Onondaga limestone revisited. *Journal of Geophysical Research B: Solid Earth*, **84**, 3576–3588.

KENT, D. V. 1985. Thermoviscous remagnetization in some Appalachian limestones. *Geophysical Research Letters*, **12**, 805–808.

KIRSCHVINK, J. L. 1978. The Precambrian-Cambrian boundary problem: paleomagnetic directions from the Amadeus Basin, Central Australia. *Earth and Planetary Science Letters*, **40**, 91–100.

KLIGFIELD, R. & CHANNELL, J. E. T. 1981. Widespread remagnetization of Helvetic limestones. *Journal of Geophysical Research*, **86**, 1888–1900.

KOPP, R. E. & KIRSCHVINK, J. L. 2008. The identification and biogeochemical interpretation of fossil magnetotactic bacteria. *Earth-Science Reviews*, **86**, 42–61.

LANCI, L. 2010. Detection of multi-axial magnetite by remanence effect on anisotropy of magnetic susceptibility. *Geophysical Journal International*, **181**, 1362–1366.

LANCI, L. & KENT, D. V. 2003. Introduction of thermal activation in forward modeling of hysteresis loops for single-domain magnetic particles and implications for the interpretation of the Day diagram. *Journal of Geophysical Research*, **108**, doi:10.1029/2001JB000944.

LANCI, L. & KENT, D. V. 2006. Meteoric smoke fallout revealed by superparamagnetism in Greenland ice. *Geophysical Research Letters*, **33**, doi:10.1029/2006GL026480.

LANCI, L., KENT, D. V. & BISCAYE, P. E. 2007. Meteoric smoke concentration in the Vostok ice core estimated from superparamagnetic relaxation and some consequences for estimates of Earth accretion rate. *Geophysical Research Letters*, **34**, doi: 10.1029/2007gl029811.

LANCI, L., DELMONTE, B., MAGGI, V., PETIT, J. R. & KENT, D. V. 2008. Ice magnetization in the EPICA-Dome C ice core: Implication for dust sources during glacial and interglacial periods. *Journal of Geophysical Research*, **113**, D14207, doi:14210.11029/12007JD009678.

LI, Y.-L., PFIFFNER, S. M. *ET AL.* 2009. Degeneration of biogenic superparamagnetic magnetite. *Geobiology*, **7**, 25–34.

LOWRIE, W. 1990. Identification of ferromagnetic minerals in a rock by coercivity and unblocking temperature properties. *Geophysical Research Letters*, **17**, 159–162.

LU, G., MCCABE, C., HANOR, J. S. & FERRELL, R. E. 1991. A genetic link between remagnetization and potassic metasomatism in the Devonian Onondaga formation, northern Appalachian basin. *Geophysical Research Letters*, **18**, 2047–2050.

MAHER, B. A. & TAYLOR, R. M. 1988. Formation of ultrafine-grained magnetite in soils. *Nature*, **336**, 368–371.

MALOOF, A. C., KOPP, R. E. *ET AL.* 2007. Sedimentary iron cycling and the origin and preservation of magnetization in platform carbonate muds, Andros Island, Bahamas. *Earth and Planetary Science Letters*, **259**, 581–598.

MCCABE, C. & ELMORE, R. D. 1989. The occurrence and origin of Late Paleozoic remagnetization in the sedimentary rocks of North America. *Reviews of Geophysics*, **27**, 471–494.

MCCABE, C. & CHANNELL, J. E. T. 1994. Late Paleozoic remagnetization in limestones of the Craven basin (northern England) and the rock magnetic fingerprint of remagnetized sedimentary carbonates. *Journal of Geophysical Research B: Solid Earth*, **99**, 4603–4612.

McCabe, C., Van der Voo, R., Peacor, D. R., Scotese, C. R. & Freeman, R. 1983. Diagenetic magnetite carries ancient yet secondary remanence in some Paleozoic sedimentary carbonates. *Geology*, **11**, 221–223.

McCabe, C., Van der Voo, R. & Ballard, M. M. 1984. Late Paleozoic remagnetization of the Trenton limestone. *Geophysical Research Letters*, **11**, 979–982.

McElhinny, M. W. & Opdyke, N. D. 1973. Remagnetization hypothesis discounted: a paleomagnetic study of the Trenton limestone, New York State. *Geological Society of America Bulletin*, **84**, 3697–3708.

Ménabréaz, L., Thouveny, N., Camoin, G. & Lund, S. P. 2010. Paleomagnetic record of the late Pleistocene reef sequence of Tahiti (French Polynesia): a contribution to the chronology of the deposits. *Earth and Planetary Science Letters*, **294**, 58–68.

Mitra, R., Tauxe, L. & Gee, J. 2011. Detecting uniaxial single domain grains with a modified IRM technique. *Geophysical Journal International*, **187**, 1250–1258, doi: 10.1111/j.1365-246X.2011.05224.x.

Molina Garza, R. S. & Zijderveld, J. D. A. 1996. Paleomagnetism of Paleozoic strata, Brabant and Ardennes Massifs, Belgium: implications of prefolding and postfolding Late Carboniferous secondary magnetizations for European apparent polar wander. *Journal of Geophysical Research, B, Solid Earth and Planets*, **101**, 15799–15818.

Moskowitz, B. M., Frankel, R. B., Bazylinski, D. A., Jannasch, H. W. & Lovley, D. R. 1989. A comparison of magnetite particles produced anaerobically by magnetotactic and dissimilatory iron-reducing bacteria. *Geophysical Research Letters*, **16**, 665–668.

Moskowitz, B. M., Frankel, R. & Bazylinski, D. 1993. Rock magnetic criteria for the detection of biogenic magnetite. *Earth and Planetary Science Letters*, **120**, 283–300.

Moskowitz, B. M., Jackson, M. & Kissel, C. 1998. Low-temperature magnetic behavior of titanomagnetites. *Earth and Planetary Science Letters*, **157**, 141–149.

Moskowitz, B. M., Bazylinski, D. A., Egli, R., Frankel, R. B. & Edwards, K. J. 2008. Magnetic properties of marine magnetotactic bacteria in a seasonally stratified coastal pond (Salt Pond, MA, USA). *Geophysical Journal International*, **174**, 75–92.

Mullins, C. E. 1977. Magnetic susceptibility of the soil and its significance in soil science – a review. *Journal of Soil Science*, **28**, 294–306.

Muttoni, G. 1995. 'Wasp-waisted' hysteresis loops from a pyrrhotite and magnetite-bearing remagnetized Triassic limestone. *Geophysical Research Letters*, **22**, 3167–3170.

Muttoni, G. & Kent, D. V. 1994. Paleomagnetism of Latest Anisian (Middle Triassic) Sections of the Prezzo Limestone and the Buchenstein Formation, Southern Alps, Italy. *Earth and Planetary Science Letters*, **122**, 1–18.

Nagata, T. & Carleton, B. J. 1987. Magnetic remanence coercivity of rocks. *Journal of Geomagnetism and Geoelectricity*, **39**, 447–461.

Néel, L. 1949. Théorie du traînage magnétique des ferromagnétiques en grains fins avec applications aux terres cuites. *Annales de Géophysique*, **5**, 99–136.

Oldfield, F., Hunt, A., Jones, M. D. H., Chester, R., Dearing, J. A., Olsson, L. & Prospero, J. M. 1985. Magnetic differentiation of atmospheric dusts. *Nature*, **317**, 516–518.

Oliva-Urcia, B. & Pueyo, E. L. 2007. Rotational basement kinematics deduced from remagnetized cover rocks (Internal Sierras, southwestern Pyrenees). *Tectonics*, **26**, 1.

Oliva-Urcia, B., Pueyo, E. L. & Larrasoana, J. C. 2008. Magnetic reorientation induced by pressure solution: a potential mechanism for orogenic-scale remagnetizations. *Earth and Planetary Science Letters*, **265**, 525–534.

Oliver, J. 1986. Fluids expelled tectonically from orogenic belts: their role in hydrocarbon migration and other geological phenomena. *Geology*, **14**, 99–102.

Özdemir, Ö. & Banerjee, S. K. 1984. High temperature stability of maghemite ($\gamma$-$Fe_2O_3$). *Geophysical Research Letters*, **11**, 161–164.

Özdemir, Ö. & Dunlop, D. J. 2006. Magnetic memory and coupling between spin-canted and defect magnetism in hematite. *Journal of Geophysical Research-Solid Earth*, **111**, 1.

Özdemir, Ö. & Dunlop, D. J. 2010. Hallmarks of maghemitization in low-temperature remanence cycling of partially oxidized magnetite nanoparticles. *Journal of Geophysical Research B: Solid Earth*, **115**, 1, doi:10.1029/2009JB006756.

Özdemir, Ö., Dunlop, D. J. & Moskowitz, B. M. 1993. The effect of oxidation of the Verwey transition in magnetite. *Geophysical Research Letters*, **20**, 1671–1674.

Potter, D. K. & Stephenson, A. 1988. Single-domain particles in rocks and magnetic fabric analysis. *Geophysical Research Letters*, **15**, 1097–1100.

Reynolds, R. L. 1990. Paleomagnetism – a polished view of remagnetization. *Nature*, **345**, 579–580.

Ripperdan, R. L., Riciputi, L. R., Cole, D. R., Elmore, R. D., Banerjee, S. & Engel, M. H. 1998. Oxygen isotope ratios in authigenic magnetites from the Belden Formation, Colorado. *Journal of Geophysical Research*, **103**, 1.

Roberts, A. P., Cui, Y.-L. & Verosub, K. L. 1995. Wasp-waisted hysteresis loops: mineral magnetic characteristics and discrimination of components in mixed magnetic systems. *Journal of Geophysical Research B: Solid Earth*, **100**, 17909–17924.

Roberts, A. P., Chang, L., Rowan, C. J., Horng, C.-S. & Florindo, F. 2011. Magnetic properties of sedimentary greigite (Fe3S4). *An update: Reviews of Geophysics*, **49**, RG1002.

Rochette, P., Fillion, G., Mattéi, J.-L. & Dekkers, M. J. 1990. Magnetic transition at 30–34 Kelvin in pyrrhotite: insight into a widespread occurrence of this mineral in rocks. *Earth and Planetary Science Letters*, **98**, 319–328.

Schlinger, C. M., Veblen, D. R. & Rosenbaum, J. G. 1991. Magnetism and magnetic mineralogy of ash flow tuffs from Yucca Mountain, Nevada. *Journal of Geophysical Research B: Solid Earth*, **96**, 6035–6052.

Scotese, C. R., Van der Voo, R. & McCabe, C. 1982. Paleomagnetism of the Upper Silurian and Lower Devonian carbonates of New York State: evidence for secondary magnetizations residing in magnetite. *Physics of the Earth and Planetary Interiors*, **30**, 385–395.

Smirnov, A. V. & Tarduno, J. A. 2001. Estimating superparamagnetism in marine sediments with the time dependency of coercivity of remanence. *Journal of Geophysical Research*, **106**, 16135–16143.

Soto, R., Villalain, J. J. & Casas-Sainz, A. M. 2008. Remagnetizations as a tool to analyze the tectonic history of inverted sedimentary basins: a case study from the Basque-Cantabrian basin (north Spain). *Tectonics*, **27**, doi: 10.1029/2007TC002208.

Stoner, E. C. & Wohlfarth, E. P. 1948. A mechanism of magnetic hysteresis in heterogeneous alloys. *Philosophical Transactions of the Royal Society of London, Series A*, **240**, 599–602.

Suk, D.-W. & Halgedahl, S. L. 1996. Hysteresis properties of magnetic spherules and whole-rock specimens from some Paleozoic platform carbonate rocks. *Journal of Geophysical Research B: Solid Earth*, **101**, 25053–25076.

Suk, D.-W., Peacor, D. R. & Van der Voo, R. 1990*a*. Replacement of pyrite framboids by magnetite in limestone and implications for paleomagnetism. *Nature*, **345**, 611–613.

Suk, D.-W., Van der Voo, R. & Peacor, D. R. 1990*b*. Scanning and transmission electron microscope observations of magnetite and other iron phases in Ordovician carbonates from east Tennessee. *Journal of Geophysical Research B. Solid Earth*, **95**, 12327–12336.

Suk, D., Voo, R. V. D. & Peacor, D. R. 1991. SEM/STEM observations of magnetite in carbonates of eastern North America: evidence for chemical remagnetization during the Alleghenian Orogeny. *Geophysical Research Letters*, **18**, 939–942.

Suk, D.-W., Van der Voo, R. & Peacor, D. R. 1993. Origin of magnetite responsible for remagnetization of early Paleozoic limestones of New York State. *Journal of Geophysical Research B: Solid Earth*, **98**, 419–434.

Sun, W.-W. & Jackson, M. J. 1994. Scanning electron microscopy and rock magnetic studies of magnetic carriers in remagnetized Early Paleozoic carbonates from Missouri. *Journal of Geophysical Research B: Solid Earth*, **99**, 2935–2942.

Symons, D. T. A., Kawasaki, K. & Pannalal, S. J. 2010. Paleomagnetic mapping of the regional fluid flow event that mineralized the Upper Mississippi Valley Zn-Pb ore district, Wisconsin, USA. *Journal of Geochemical Exploration*, **106**, 188–196.

Tarduno, J. A. 1995. Superparamagnetism and reduction diagenesis in pelagic sediments: enhancement or depletion? *Geophysical Research Letters*, **22**, 1337–1340.

Tarduno, J. A. & Myers, M. 1994. A primary magnetization fingerprint from the Cretaceous Laytonville Limestone: further evidence for rapid oceanic plate velocities. *Journal of Geophysical Research B, Solid Earth*, **99**, 21691–21703.

Tauxe, L., Mullender, T. A. T. & Pick, T. 1996. otbellies, wasp-waists, and superparamagnetism in magnetic hysteresis. *Journal of Geophysical Research B, Solid Earth*, **101**, 571–583.

Till, J. L., Jackson, M. J., Rosenbaum, J. G. & Solheid, P. 2010. Magnetic properties in an ashflow tuff with continuous grain size variation: A natural reference for magnetic particle granulometry. *Geochemistry, Geophysics, Geosystems*, **12** (Q07Z26), doi: 10.1029/2011GC003648.

Tohver, E., Weil, A. B., Solum, J. G. & Hall, C. M. 2008. Direct dating of carbonate remagnetization by 40Ar/39Ar analysis of the smectite–illite transformation. *Earth and Planetary Science Letters*, **274**, 524–530.

Trindade, R. I. F., D'Agrella, M. S., Babinski, M., Font, E. & Neves, B. B. B. 2004. Paleomagnetism and geochronology of the Bebedouro cap carbonate: evidence for continental-scale Cambrian remagnetization in the Sao Francisco craton, Brazil. *Precambrian Research*, **128**, 83–103.

Van der Voo, R. 1990. The reliability of paleomagnetic data. *Tectonophysics*, **184**, 1–9.

Verwey, E. J. & Haayman, P. W. 1941. Electronic conductivity and transition point in magnetite. *Physica*, **8**, 979–982.

Walton, D. 1980. Time-temperature relations in the magnetization of assmblies of single-domain grains. *Nature*, **286**, 245–247.

Walz, F. 2002. The Verwey transition – a topical review. *Journal of Physics: Condensed Matter*, **14**, R285–340.

Weil, A. B. & Van der Voo, R. 2002. Insights into the mechanism for orogen-related carbonate remagnetization from growth of authigenic Fe-oxide: A scanning electron microscopy and rock magnetic study of Devonian carbonates from northern Spain. *Journal of Geophysical Research*, **107**, 1, doi:10.1029/2001JB000200.

Wohlfarth, E. P. & Tonge, D. G. 1957. The remanent magnetization of single-domain ferromagnetic particles. *Philosophical Magazine*, **2**, 1333–1344.

Wolfers, P., Fillion, G., Ouladdiaf, B., Ballou, R. & Rochette, P. 2011. The Pyrrhotite 32 K magnetic transition. *Solid State Phenomena*, **170**, 174–179.

Woods, S. D., Elmore, R. D. & Engel, M. H. 2002. Paleomagnetic dating of the smectite-to-illite conversion: testing the hypothesis in Jurassic sedimentary rocks, Skye, Scotland. *Journal of Geophysical Research*, **107**, doi: 10.1029/2000JB000053.

Worm, H.-U. 1998. On the superparamagnetic-stable single domain transition for magnetite, and frequency dependence of susceptibility. *Geophysical Journal International*, **133**, 201–206.

Worm, H.-U. & Jackson, M. 1999. The superparamagnetism of Yucca Mountain Tuff. *Journal of Geophysical Research B: Solid Earth*, **104**, 25415–25425.

Xu, W., Van der Voo, R. & Peacor, D. R. 1998. Electron microscopic and rock magnetic study of remagnetized Leadville carbonates, central Colorado. *Tectonophysics*, **296**, 333–362.

Zegers, T. E., Dekkers, M. J. & Bailly, S. 2003. Late Carboniferous to Permian remagnetization of Devonian limestones in the Ardennes: role of temperature, fluids, and deformation. *Journal of Geophysical Research*, **108**, doi: 10.1029/2002JB002213.

Zwing, A., Matzka, J., Bachtadse, V. & Soffel, H. C. 2005. Rock magnetic properties of remagnetized Palaeozoic clastic and carbonate rocks from the NE Rhenish massif, Germany. *Geophysical Journal International*, **160**, 477–486.